2021

Investigating ecogeographic variation in superior and functional ethmoidal breadth in internal nasal dimensions

BOSTON UNIVERSITY

SCHOOL OF MEDICINE

Thesis

INVESTIGATING ECOGEOGRAPHIC VARIATION IN SUPERIOR AND FUNCTIONAL ETHMOIDAL BREADTH IN INTERNAL NASAL DIMENSIONS

by

CAROLINE REID GRACE

B.A., Baylor University, 2018

Submitted in partial fulfillment of the

requirements for the degree of

Master of Science

2021

Approved by

First Reader ____
Sean D. Tallman, Ph.D.
Assistant Professor of Anatomy & Neurobiology

Second Reader ____
Scott D. Maddux, Ph.D.
Assistant Professor of Anatomy
University of North Texas Health Science Center

ACKNOWLEDGMENTS

None of this would have been possible without the leadership of Dr. Scott Maddux, who was not only an advocate and role model throughout the research and writing process but also a mainstay in an overall chaotic year. Thank you for my access to the cranial material, your knowledge on the collections, and our writing efforts. Cecelia Schaefer's preliminary results paved the way for continued investigation and inspired the optimism to keep mining for data. I would also like to thank the Comparative Morphology Lab at UNT HSC's Center for Anatomical Science for sharing their time, space, and geomorphing talents with me, and our weekly journal clubs for expanding my scientific interests and challenging my thought process. Thank you to my academic advisor, Dr. Keith Tornheim, for replying to my e-mails at all hours and providing educational and professional guidance. Thank you to Dr. Sean Tallman for taking a risk on editing the writing of a first-time anthropologist. Thank you to the archivists who provided my seamless access to human history through the careful preservation and organization of hundreds of centuries old skulls. I greatly indebted to the individuals who facilitated data collection at the American Museum of Natural History (Gisselle Garcia), National Museum of Natural History (Dr. David Hunt) and the University of Pennsylvania's Open Research Scan Archive (Drs. Janet Monge and Tom Schoenemann). Thank you Dr. Lauren Butaric and Tarah Marks for assistance with technical aspects of this project. Thank you to my family, friends, and dogs for listening to the ramblings of my research before it became a coherent document.

INVESTIGATING ECOGEOGRAPHIC VARIATION IN SUPERIOR AND FUNCTIONAL ETHMOIDAL BREADTH IN INTERNAL NASAL DIMENSIONS

CAROLINE REID GRACE

ABSTRACT

Superior Ethmoidal Breadth (SEB = the maximum breadth between the left and right frontoethmoidal sutures) has been widely employed by anthropologists as a proxy for internal nasal airway dimensions since it is easily measured without imaging. SEB is also commonly argued to evince climatic adaption in modern humans, as populations living in cold-dry environments predictably exhibit narrower SEB dimensions than those inhabiting tropical environments. However, given uncertaintiy regarding its relationship with internal nasal anatomy, the accuracy of SEB as a proxy for airway dimensions remains questionable. Here, I evaluate the correlation between SEB and internal airway dimensions using linear measurements collected on CT scans from a mixed-sex sample of human crania (n=215) ancestrally derived from sub-Saharan Africa, the Arctic Circle, East Asia, and Europe. My results demonstrate that SEB is often located superior to the anatomcial roof of the nasal passages but is highly correlated ($R= 0.8119$, $p<0.0001$) with ethmoidal breadth taken at the functional level of the upper airways (i.e., functional airway breadth [FEB]). ANOVA results indicate, in addition to significant differences in SEB ($\chi^2 = 82.20$, $p<0.0001$), regional differences also exist for FEB ($\chi^2 = 54.21$, $p<0.0001$) and its components: the combined superior and superior common meatal breadths ($\chi^2 = 19.03$, $p< 0.0001$) and ethmoid air cell (EAC) breadth ($\chi^2 = 27.67$, $p<0.0001$). Further, following theoretical expecations, the African-derived sample

generally exhibits the widest internal nasal dimensions and the Arctic-derived sample the narrowest. Specifically, the Arctic sample exhibits significantly narrower airway breadths compared to all other groups. Conversely, the African sample possesses significantly wider EAC breadths comapred to all other groups. Cumulatively, these results empirically support use of SEB as proxy for upper nasal airway breadth and bolster claims that clinal variation in internal airway dimensions across human populations is likely attributable to climatic factors.

TABLE OF CONTENTS

LIST OF TABLES

LIST OF FIGURES

LIST OF ABBREVIATIONS

ANOVA .... Analysis of Variance

biEAC .... Bilateral Ethmoidal Air Cells

CG .... Crista Galli

CMB .... Common Meatal Breadth

CT .... Computer Tomography

EAC .... Ethmoid Air Cell

FEB .... Functional Ethmoidal Breadth

IT .... Inferior Turbinate

MT .... Middle Turbinate

NB .... Nasal Breadth

NH .... Nasal Height

OMC .... Osteomeatal Complex

SA/V .... Surface Area-to-Volume

SEB .... Superior Ethmoidal Breadth

SCMB .... Superior Common Meatal Breadth

SMB .... Superior Meatal Breadth

ST .... Supreme Turbinate

INTRODUCTION

The empirical study of human adaptation is essential to the understanding of disease etiology as it relates to anatomy, genetics, physics, and ecology. While multiple evolutionary mechanisms, including both genetic drift and natural selection, have played predominant roles in human evolution, physical traits that demonstrably interact with environmental factors, such as temperature and humidity, are widely assumed to have been influenced by climatic adaptation. Anthropologists began recognizing strong statistical associations between nasal morphology and climate over 100 years ago (Thomson, 1913; Thomson & Buxton, 1923). Through advances in technology, such as 3D imaging and dynamic airflow studies, scientists have increasingly been able to not only describe the anatomy of the nasal structures and quantify its ability to heat and humidify inspired air (Cole, 1953a, 1953b; Doorly et al., 2008; Elad et al., 1993; Hildebrandt et al., 2013; Keck et al., 2000a, 2000b; Keyhani et al., 1995; Uliyanov, 1998; Walker et al., 1961; Wolf et al., 2004), but also examine the impact of nasal morphological variation on air conditioning physiology (Churchill et al., 2004; Elad et al., 2008; Ma et al., 2018; Naftali et al., 2005; Zhao & Jiang, 2014).

However, while generally incorporating large and geographically diverse samples, due to methodological limitations, anthropological studies have historically focused predominantly on external nasal morphology (Maddux et al., 2017). Indeed, prior to advancements in medical imaging (e.g., computed tomography, magnetic resonance imaging) and multivariate statistics (e.g., 3D geometric morphometrics) permitting accurate visualization and quantification of internal nasal anatomy, early studies were effectively unable to access certain areas — like the narrow and fragile recesses of the internal nose — increasing reliance on the assumption that external features were inherently representative of inner variation (Yokley, 2009; Noback et al., 2011; Maddux et al., 2017). Moreover, early anthropological studies of the human nose were, unfortunately, often biased by the prevailing political/social climate of the time, leading to typological analysis of geographically-patterned nasal morphology being employed to legitimize racist pseudoscience, such as biological determinism (Belkhir & Duyme, 1998; Blakey, 1999).

Scientific racism, the false belief that race is foundationally biological and quantifiable, is resilient in foundational literature for anthropology and neglects to account for the myriad of social and environmental factors that create biological realities associated with race (Charles, 1930; Gravlee, 2009; Ackermann, 2019). Extensive studies on genetic and craniometric data as a reflection of population structure and history of neutral traits show roughly 10% of total species variation exists between major regions, 5% among localities, and 85% within local populations (Relethford, 2002). Meanwhile, the distribution for skin color has been affected differentially by natural selection, and tells little about global population history and relationships (Relethford, 2009). Racial classifications are inadequate to describe anatomical differences or human biological variation, and their employment prevents anthropology from not only becoming a more quantitative and analytical discipline but also empowers stereotypes that prove more harmful and less accurate (Ackermann, 2019; Blakey, 1999). Population history, adaptation, neutral evolutionary forces, and environment have all shaped the distribution of the phenotypic variation that contribute to continuous and – often polygenic – traits, such as nose size and shape (Evteev et al., 2014, 2015). Especially considering specific environments along latitude, such as clinal variation in skin pigment or nasal morphology, there contains more diversity within bureaucratic races than between them (Corey et al., 1998).

The nasal aperture (Figure 1) has garnered the most anthropological attention, with numerous studies investigating the relationship between climate and nasal height, breadth, and protrusion (Crognier, 1981a, 1981b; Davies, 1932; Franciscus & Long, 1991; Hubbe et al., 2009; Leong & Eccles, 2009; Thomson, 1913; Thomson & Buxton, 1923; Weiner, 1954; Wolpoff, 1968). Perhaps the most influential study was that of Weiner (1954) who first demonstrated a strong positive correlation (r=0.82) between the nasal index (a measure of relative nasal breadth calculated as nasal breadth/nasal height x100) and average annual absolute humidity. More recently, Roseman (2004) has shown that, while variation in both nasal height and nasal breadth among regional populations are attributable to climatic adaptation, nasal height appears to have been influenced by selection to a greater degree (Roseman, 2004). Potentially more importantly, Yokley (2009) demonstrated the nasal index is not strongly correlated with internal dimensions.

While the exact role of external variation in heat and moisture exchange continues to be contested, it is commonly believed that the width of the external nose is inversely correlated with the ability to condition air and the height positively correlated, which individually contribute to ecogeographic distribution of nasal morphology (Franciscus & Long, 1991; Inthavong et al., 2007; Wolpoff, 1968). However, it is the internal function of the nose to sufficiently modify environmental air which is necessary to protect the lungs from thermal damage, desiccation, and infection (Cole, 1982; Eccles, 2002), and contributes to overall homeostatic thermoregulation (Havenith, 2005; Hildebrandt et al., 2013). Therefore, investigations into the internal nasal structures have revealed how pivotal climate is for human nasal evolution (Bastir et al., 2011; Carey & Steegmann, 1981; Davies, 1932; Evteev et al., 2014; Franciscus & Long, 1991; Franciscus & Trinkaus, 1988; Harvati & Weaver, 2006; Hubbe et al., 2009; Maddux et al., 2017; Maddux et al., 2016; Noback et al., 2011; Thomson, 1913; Thomson & Buxton, 1923; Weiner, 1954; Wolpoff, 1968; Yokley, 2009; Zaidi et al., 2017).

Figure 1. The Anatomy of the Nasal Cavity

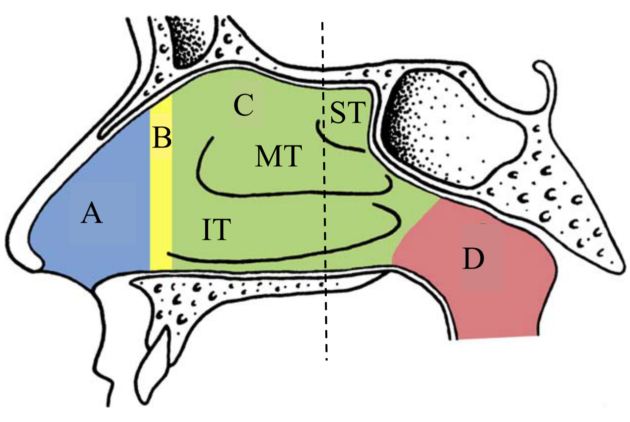

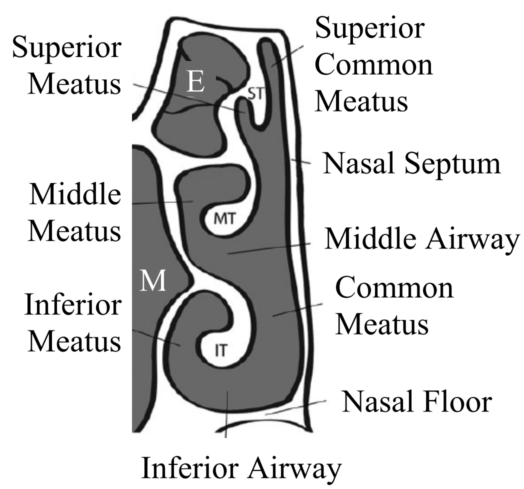

Left: Medial view of nasal passages and four morphofunctional units. A) External pyramid, including vestibule, concave isthmus, and anterior cavum; B) nasal aperture; C) internal nasal fossa with inferior (IT), middle (MT), and superior (ST) turbinates emptying into the posterior cavum; D) nasopharynx. Taken from Maddux et al. (2016, page 104). **Right: Coronal view of internal nasal fossa's turbinate and meatus structure.** Cross-section from the plane indicated by the dotted lines in the left image. Maxillary sinus (M) and ethmoidal air cells (E) border the turbinates. Adapted from Marks et al. (2019, page 2).

Nasal Cavity Shape and Function

Physics of Air Conditioning

Upon inspiration, air is heated and humidified at the respiratory mucosa (Figure 2). First, heat is transferred through convection, as thermal and osmotic pressure gradients exponentially drive evaporation to near-complete water vapor saturation in the nasopharynx (Walker et al., 1961). Under a wide range of ambient conditions (-30 to 25 °C and 35–50% relative humidity), inspired air has been shown to be warmed to 31–34 °C and almost fully saturated with water vapor by the time it reaches the nasopharynx (Cole, 1953a, b, 1954; Inglestedt, 1956; Keck et al., 2000a). The process of heating and humidifying inspired air continues minimally as needed in the pharynx, larynx, and trachea; and further airflow alterations, such as turbulence, pressure, and direction, are made as it passes to the lungs, where air is 100% saturated (44 g/m3) at body temperature (37°C) (Mlynski et al., 2001; Segal et al., 2008). Since the majority of air conditioning occurs in the inspiratory phase, much of the investigation into nasal variation has prioritized inflow.

During expiration, air is cooled by heat loss during turbulent convection, so that the heat can return to cooled mucosa. Meanwhile, the moisture and latent heat of vaporization is recaptured by the mucosa through condensation (Mariak et al., 1999; Figure 2). Cole (1982a) estimated that in more ambient conditions approximately one-third of the heat and water transferred to inspired air is recovered during expiration, whereas at temperatures as low as -30°C over half of the transferred heat and water is salvaged. Therefore -- even in low temperatures -- inspired air will have greater convective cooling, and low humidity will produce greater evaporative cooling, both facilitating a greater recovery of heat and water in inspired air opposed to a greater loss of heat and water in expired air.

Figure 2. Respiratory cycle of conditioning air.

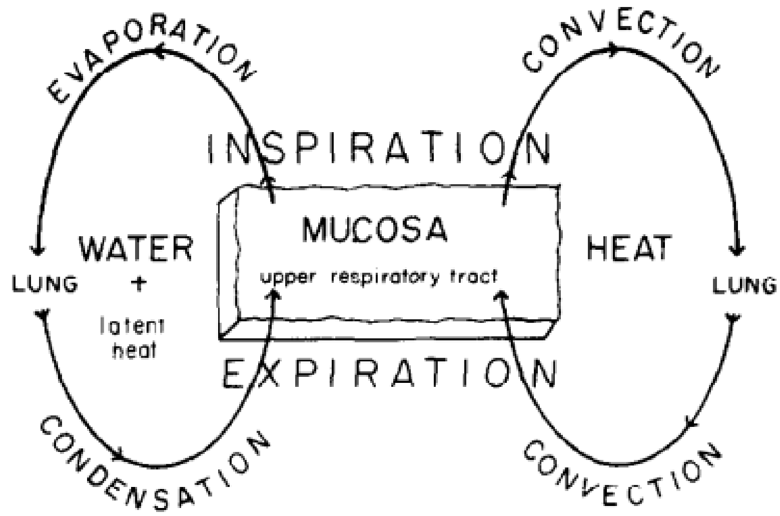

Taken from Walker et al. (1961, page 261). Upon inspiration, the nasal mucosa undergoes convection and evaporation to retain heat and moisture. Upon expiration, the nasal mucosa again undergoes convection to retain heat, in addition to condensation to retain moisture.

Conditioning air is distinctly affected by the two biomechanical types of airflow: turbulent and laminar. Laminar airflow, characterized by smooth and streamlined airflow, minimizes contact between respired air and the mucosa-lined peripheries of the nasal passages, resulting in a lower overall potential for heat and moisture transfer. In contrast, turbulent airflow results in increased circulation of respired air in the nasal passages which causes more of the airstream to contact nasal mucosa and facilitating heat and moisture transfers (Churchill et al., 2004). Generally, more platyrrhine noses (i.e., relatively shorter and wider) are believed to be suited for laminar flow; whereas, more leptorrhine noses (i.e., relatively taller and narrower) are thought to enhance turbulence and thus air-conditioning (Churchill et al., 2004; Thomson & Buxton, 1923).

However, to date, these functional assertions have garnered minimal empirical support (Churchill et al., 2004; Zhao & Jiang, 2014), mainly due to methodological limitations in accurately testing these proposed form-function relationships (Marks et al., 2019). Meanwhile, NB measurements are significantly correlated with their nasal cavity size (Yokley, 2009) and will require a more complex understanding of their functional anatomy.

Anatomy and Physiology of Nasal Airways

During inspiration and expiration, the various structural components of the nasal complex (see Figure 1) fundamentally alter the pattern and velocity of air as it passes through the upper respiratory tract, which ultimately mediates contact between respired air and the nasal mucosa. While the internal nasal fossa (Figure 1 part C) is commonly referred to as the "functional area" because it is where the majority of contact between respired air and nasal mucosa occurs (Mlynski et al., 2001; Noback et al., 2011), other areas of the nose (e.g., nasal valve, nasophaynx) likely play important roles in regulating the directionality and velocity of the airstream, which contributes to air-mucosal contact (Churchill et al., 2004; Cole, 2000; Doorly et al., 2008; Elad et al., 1993; Hildebrandt et al., 2013; Zhao & Jiang, 2014). Still, to a large extent, the overall efficacy of respiratory air-conditioning remains predominantly attributable to air-mucosal contact mediated by the anatomy of the internal nasal fossa (Elad et al., 2008; Keyhani et al., 1995; Na et al., 2012; Yokley, 2009).

<u>Skeletal Components of the Nasal Fossa</u>

To better understand the anatomy of the airway, it is important to be aware of the embryology of the turbinates and sinuses that define the boundaries of the meatal breadths. There are six embryological lamellae pairs that form from the lateral nasal wall that fuse into four lamellae early in fetal development, which give rise to important structures in the nose (Cole, 1982). The first lamella forms the uncinate process, the second the bulla ethmoidalis, the third the middle turbinate (MT), the fourth the superior turbinate (ST) and the fifth (persistent from development in 10% of the population) will result in the presence of a supreme turbinate (Psaltis & Wormald, 2019; Figure 1). Inhaled air is channeled through these thin, conch-shaped, erectile structures prior to funneling to the nasophaynx (Cobzeanu et al., 2014; Naftali et al., 2005; Figure 1). All turbinates arise from the cartilaginous nasal capsule, and every turbinate except for the inferior turbinate (IT) articulate with the centrally located ethmoid bone, where olfactory sensation, humidification, ventilation, phonation, and sinus drainage collide in the delicate, sponge-like cranial bone that is approximately the size of an ice cube (Gibelli et al., 2018; Maroldi et al., 2005). The ethmoid bone is then divided into three parts: the horizontal (cribriform) plate, from which the MT and ST hang in the coronal plane; the vertical plate, extending from the crista galli (CG) through the nasal septum (NS) in the sagittal plane; and finally, the lateral ethmoidal labyrinth, containing sinuses called ethmoidal air cells (EAC) (Maroldi et al., 2005). The size, functional variety, and difficult to access anatomy of the ethmoid bone has provided several obstacles and opportunities for studying the superior internal airway.

Each turbinate develops via endochondral ossification and divide each nasal passage into further subdivided airways called meatuses located inferolateral to each turbinate (Lang, 1989). Most recently, it has been demonstrated that environmental temperatures can directly alter cartilage development (and therefore endochondral bone morphology) through cell proliferation and matrix production (Serrat et al., 2015). This may influence the development of surrounding intramembranous-derived nasal structures, such as the nasal bones, during ontogeny (Holton et al., 2018). The nasolacrimal duct drains into the inferior meatus; the anterior ethmoid cells, maxillary sinus, ethmoid bulla, and frontal sinus all drain into middle meatus; and the posterior ethmoid cells and sphenoid sinus drain into superior meatus (SM) (Maroldi et al., 2005). The meatuses each connect medially to a vertically elongated airway adjacent to the NS of the vertical ethmoidal plate —the common meatus (CM) (Sahin-Yilmaz & Naclerio, 2011; Figure 1). These three planes and three parts of the ethmoid bone are primarily described for the respiratory purposes in this study, although there are many other pivotal anatomical structures and functions.

While superior and supreme meatuses are extensively covered in olfactory mucosa, both the middle and inferior turbinates are predominantly covered by respiratory mucosa, which differs from the former primarily due to its multitude of cells suited for mucus production (Maroldi et al., 2005; Tos, 1986). These goblet and seromucous cells allow for more air and heat exchange with the nasal mucosa despite increased resistance, which both moisturizes and filters particulates, contributing to more effective long-term inspiratory conditioning (Cole, 1982). Goblet cells are also contained throughout the paranasal sinuses, such as the EAC. While these pneumatizations do not directly contribute to airflow like the meatuses, as they primarily function in innate immunity, EAC increases air volume alongside the superior and middle concha for increased residence time (Inthavong et al., 2007). In addition, pneumatization increases with age until stabilization in adulthood, so structures like the EAC have gradually changing morphology that contribute to the variety of factors the effect airflow.

Airflow changes from anatomical causes are primarily affected by the spontaneous congestion and decongestion of nasal venous sinuses, often referred to as the nasal cycle (Holton et al., 2018; Walker et al., 1961). The nasal mucosa is invested with a rich vascular supply, including fenestrated capillaries that further facilitate evaporation of water into the airway, and numerous arteriovenous anastomoses, which likely support mucosal temperature regulation via vascular countercurrent heat exchange. Although all parts of the respiratory tract are capable of temperature and moisture modification through its immense vascularization, the nasal passages are responsible for the majority of heating and humidifying (Cauna, 1982; Cole, 1982; Inglestedt, 1956; Keck et al., 2000b; Walker et al., 1961). This mucosa also overlays extensive venous capacitance vessels, or sinuses, which contribute to the nasal erectile tissues. Changes in blood volume in these vessels results in variable swelling of the mucosa, thus modifying the size and shape of the nasal airways—and ultimately—the speed, volume, and direction of nasal airflow (Cauna, 1982; Churchill et al., 2004). For example, vasoconstriction decreases airflow resistance. Yokley (2009) convincingly argued that fully decongested morphology is representative of the body undergoing exertion, which would imply selective pressures affect turbinate morphology in addition to climate-mediation.

The meatuses' position and spatial relationships within the boundaries of the ethmoidal air cells are extremely important for air cycling and conditioning. Previous airflow studies have shown that substantially more of the inspiratory volume of air passes through the CM compared to the inferior meatus especially in the anterior half of the nasal passage (Inthavong et al., 2007; Keyhani et al., 1995). Airflow velocity in the upper half of the nasal cavity is also considerably slower and potentially more turbulent (Ma et al., 2018; Zhao & Jiang, 2014) than along the nasal floor, which could affect the air-conditioning capabilities of the middle and upper airways with increased residence time in contact with mucosa. The subsequent narrowing of the common meatus toward the middle of the nasal passage then functions as funnel with increasing the airflow velocity between the turbinate and the septum, and thus, facilitating greater transfer of heat and moisture from the mucosa to inspired air via (Churchill et al., 2004; Hildebrandt et al., 2013; Marks et al., 2019). All of this occurs within the anterior compartment of the ethmoid bone, where variability across climatic variables is more pronounced than the posterior (Bastir et al., 2011; Maddux et al., 2017). The duration of time in the nasal cavity (residence time) (Inthavong et al., 2007; Noback et al., 2011) is primarily influenced by increased fossa length rather than the SA/V ratio (Yokley, 2009). Ultimately, the height and breadth of the nasal cavity influence SA/V whereas length mainly impacts residence time (see Maddux et al 2017; Noback et al., 2011; Yokley, 2009 for further discussion). Therefore, while the velocity and resistance of airflow affects conditioning, they are less likely to be the influencers.

Variation in the Nasal Fossa

Variable attachments between the lamellae previously discussed can result in a difficulty discerning anatomy. For example, the size of the frontal recess in the nasal cavity (anteriorly bounded by the maxilla at the height of the cribriform plate) determines not only the size of certain air cells, such as a the agger nasi, but also the attachment location of the uncinate process (Psaltis & Wormald, 2019). Visualized on CT, these structures can resemble both the EAC and MT respectively if the airway anatomy is missing or broken. Classification of these frontal air cells has been ongoing since 1995, when Kuhn began organizing the cells seen in the frontal recess initially for guiding sinus dissection and reconstruction surgery as treatment chronic sinusitis patients (Psaltis & Wormald, 2019). In addition, excessive narrowing of the airways can manifest pathologically and often must be repaired procedurally. Specifically, it is concha bullosa, or the pneumatization/presence of air cells in the turbinates unilaterally or bilaterally, that can create large blockages for both airflow and the normal drainage of paranasal sinuses (Nicoleta et al., 2015). Concha bullosa is often associated with contralateral nasal septal deviation, further complicating normal nasal function (Cobzeanu et al., 2014; (Gibelli et al., 2018; Maroldi et al., 2005). Septal deviation is normally the cause of structural nasal obstruction, whereas lateral wall abnormalities are rare and usually iatrogenic (Cole, 2000; Earwaker, 1993; Uliyanov, 1998). Other common variations in the osteomeatal complex (OMC) include septal and uncinate bulla, which occur in a majority of humans with varying severity (Earwaker, 1993).

While narrowing of these structures can be pathologic, it has also been show that narrowing nasal passages facilitates heat and moisture exchange by increasing the SA/V ratio (Lindemann et al., 2009; Schmidt-Nielsen et al., 1970; Schroter & Watkins, 1989). Population-level differences in turbinate size and shape could represent one mechanism by which human populations have adapted to climate-mediated pressures for intranasal heat and moisture exchange. This variation in turbinate morphology has been demonstrated to coordinate with the outer walls of the nasal passage as if to influence the functional dimensions of the nasal airways (Marks et al., 2019). Internal nasal fossa is the only component of the nasal complex which has been shown to demonstrate an ecogeographic pattern of variation consistent with adaptation to climatic conditions (Maddux et al., 2017). However, unlike the encapsulating walls of the nasal cavity (Bastir et al., 2011; Charles, 1930; Franciscus, 1995; Fukase et al., 2016; Maddux et al., 2017; Noback et al., 2011), ecogeographic variation in human nasal turbinate morphology may display more plasticity due to the capacity to remodel in response to environmental and biomechanical factors (Marks et al. 2019). This can make it difficult to accurately translate the findings between *in* and *ex vivo* studies of crania.

Among the turbinates, it has been noted that regional differences in breadth are significantly more pronounced in the superior nasal cavity (e.g., ethmoidal) compared to the inferior areas (Franciscus, 1995; Maddux et al., 2017). Humans follow a similar pattern of geographically-mediated inferior turbinate morphology that is generally attributed to climatic and thermoregulatory pressures in other mammalian taxa (Marks et al., 2018; Schmidt-Nielsen et al., 1970; Van Valkenburgh et al., 2004). In addition to the encapsulating bony walls of the nasal cavity (Bastir et al., 2011; Butaric & Klocke, 2018; Franciscus, 1995; Fukase et al., 2016; Holton et al., 2013), the inferior nasal turbinates also contribute to an overall pattern of ecogeographic variation within the human nasal complex (Marks et al., 2019). In particular, as the skeletal morphology of the nasal cavity closely approximates decongested in vivo anatomy (Yokley, 2009), and several studies suggest that turbinate morphology covaries with that of the surrounding nasal passage walls to produce region-specific differences in the functional nasal airways (Marks et al., 2019).

The Role of Climate

Adaption to climatic pressures is a widely accepted evolutionary process (Bastir et al., 2011; Carey & Steegmann, 1981; Davies, 1932; Evteev et al., 2014; Franciscus & Long, 1991; Franciscus & Trinkaus, 1988; Harvati & Weaver, 2006; Hubbe et al., 2009; Maddux et al., 2017; Maddux et al., 2016; Noback et al., 2011; Thomson, 1913; Thomson & Buxton, 1923; Weiner, 1954; Wolpoff, 1968; Yokley, 2009; Zaidi et al., 2017). Indeed, it has been estimated that climate accounts for approximately 35% of the total variance of physical features between human populations (Crognier, 1981a). A number of ecogeographic rules related to evolutionary adaptations to climate have been proposed, with Bergmann's (1847) and Allen's (1877) rules being by far the best known.

Collectively, Bergmann's and Allen's rules states that, in warm climates, a more linear and smaller body form facilitates heat dissipation by increasing the amount of skin surface area relative to the overall volume of the organism. In contrast, these rules suggest that in cold climates, more rounded and larger bodies better retain heat by minimizing this SA/V ratio (Allen, 1977; Bergmann, 1847).

In addition to Bergmann's and Allen's rules, the role of the nasal passages in thermoregulation has also been extensively investigated (Davies, 1932; Hildebrandt et al., 2013; Kim & Maddux, 2018; Mariak et al., 1999). In comparison to other mammals, the human nose has several important anatomical and physiological characteristics. First, the human nose lacks the specialized carotid rete present for the cooling purpose in some animals (Schroter & Watkins, 1989; Van Valkenburgh et al., 2004). This structure efficiently exchanges heat from arterial blood traveling to the brain to venous blood traveling away from the nasal passages in order to keep the brain cooler than body temperature (Mariak et al., 1999). Second, the surface of the human nose is usually small compared to other mammals of similar body size, theoretically reducing its potential influence on overall body temperature regulation (Weiner, 1954). Therefore, studies of the nasal cavity have typically focused on nasal conditioning of air during inspiration rather than potential thermoregulatory impacts on core body temperature. However, as breathing in hot and humid environments requires virtually no warming or humidifying of inspired air (Noback et al., 2011; Maddux et al., 2016), it has previously been suggested that a low nasal SA/V ratio, along with reduced airway resistance and more laminar flow, could actually serve as an evolutionary mechanism to functionally reduce the recapture of heat and humidity during expiration (Noback et al., 2011; Maddux et al., 2016; 2017; Marks et al., 2019). Thus, given reduced demands for inspiratory modification in tropical environments (Table 1), it has been surmised that expiratory heat elimination for thermoregulation could be a greater selective pressure on nasal morphology in environments such as tropical rainforests (Maddux et al., 2016; Marks et al., 2019) where passive evaporative cooling via sweating is less effective (Cole, 1982a; Mariak et al., 1999).

In contrast to hot-humid environments, colder air, with its inherently reduced ability to support water vapor, physiological requires inspiratory modification in order to adequately prepare respired air for entry into the lungs (Table 1). Accordingly, previous studies have demonstrated that humans indigenous to the Arctic Circle possess nasal passages that are relatively tall and narrow, with larger and more medially projecting turbinates compared to equatorial populations (Noback et al., 2011; Maddux et al., 2017; Marks et al., 2019). Cumulatively, this overall anatomical architecture acts to increase the relative mucosal surface areas of the nasal cavities relative to the volume in respired air, theoretically enhancing heat and moisture transfer from the nasal mucosa to cold-dry environmental air during inspiration (Evteev et al., 2014; Franciscus, 1995; Fukase et al., 2016; Noback et al., 2011; Maddux et al., 2017).

Importantly, of the various measurements that have been employed to assess ecogeographic variation in nasal passage morphology, superior ethmoidal breadth (SEB), the maximum breadth between the left and right frontoethmoidal sutures, has repeatedly been shown to exhibit exceptionally strong statistically correlations with climatic variables (Franciscus, 1995; Noback et al., 2011; Evteev et al., 2014; Maddux et al., 2017). Specifically, populations living in cold-dry environments predictably exhibit narrower SEB dimensions than those inhabiting tropical environments (Figure 3). As a consequence, SEB is widely argued to evince climatic adaptation in the upper nasal airways among modern humans. However, SEB itself actually spans three anatomical features: the CM, SM (functional airways) and the EAC (non-airway). Therefore, the accuracy of SEB as a proxy for airway dimensions remains questionable. However, it has yet to be evaluated whether the internal superior structures, such as the SM and SCM breadths would be similarly subjected to evolutionary pressures in the presence of clear geographic clines in the overall size and anterior nasal shape.

Table 1. Overview of Air-Conditioning Demands in Different Climate Types

Climate	Regional Examples	Respiratory Demands	Anticipated FEB
Tropical	Equatorial Africa	No heat or humidity preservation needed; prioritizes cooling on expiration, enhanced turbulence	Wider internal airways
Temperate	Europe, East Asia	Seasonal fluctuations between either extreme; moderate	Intermediate
Cold-dry	Arctic Circle	Warming and humidification needed; conservation of heat and moisture on expiration, minimal turbulence	Narrower internal airways

Figure 3. Linear Regression of SEB across climates.

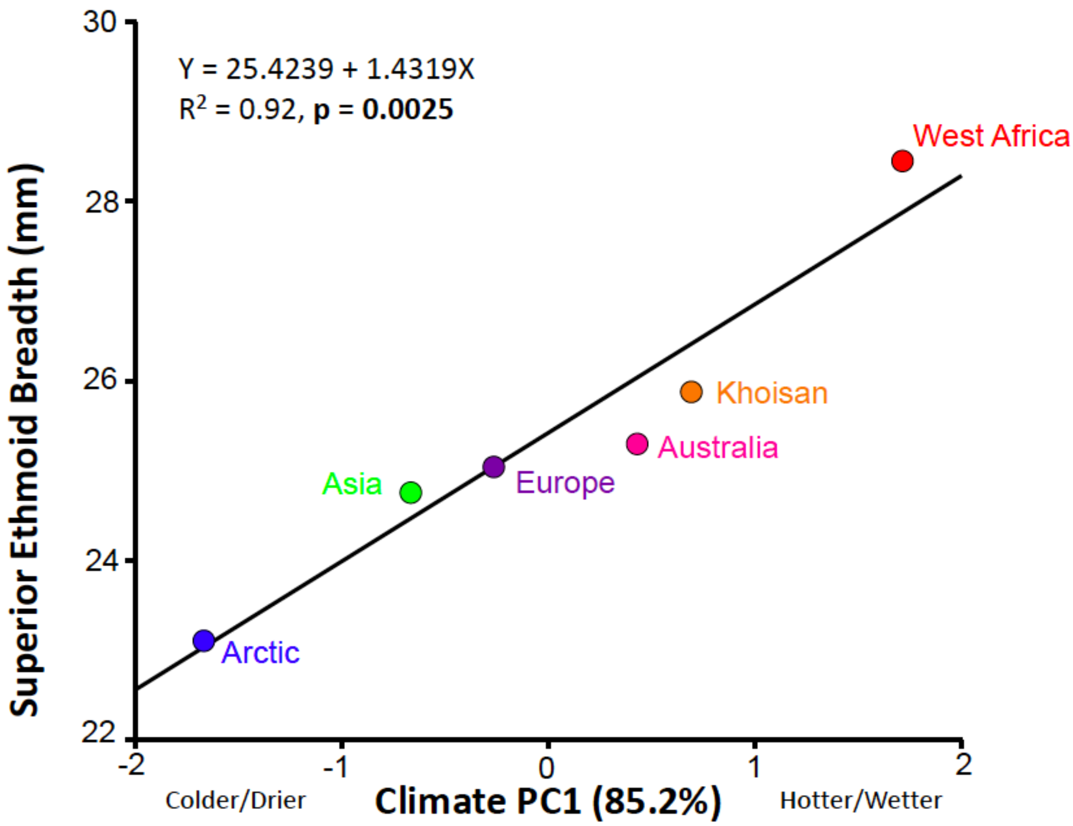

Includes regions that will not be evaluated in this study, specifically Australia and Khoisan, but are provided for perspective. Derived from Maddux et al. (2017, page 114) and originally formatted by Schaefer & Maddux (2019).

Objectives

1. Assess the reliability of SEB as an osteometric proxy for superior nasal airway dimensions.

   Hypothesis 1: SEB will be highly correlated to the ethmoidal breadth taken at the functional level of the upper airways (i.e., functional airway breadth [FEB]), which includes the superior airway structures, SM and SCM, and non-airway spaces, EAC.

2. Determine whether actual internal airway dimensions following predicted ecogeographic patterns.

   Hypothesis 2: Populations indigenous to colder-drier climates will exhibit narrower superior nasal airway (SCM and SM) dimensions compared to those from warmer-wetter environments.

Justification of Need

While SEB has historically been employed as an osteometric proxy for upper airway dimensions, it is anatomically superior to the roof of the internal nasal cavity and thus above the actual airways. In order to determine if this manual measurement is an accurate representation of the superior breadth that comes into contact with inspired air, this study will visualize crania through CT, apply previous standards for measuring the nasal aperture, and develop a methodology for obtaining landmarks of internal airways at the level of the ethmoid.

MATERIALS AND METHODS

Samples

To assess regional differences in upper internal nasal morphology, 18 landmarks and 16 measurements were collected from CT scans of a mixed-sex sample of modern human crania (n=215) indigenous to four distinct regions: Equatorial Africa, the Arctic Circle, East Asia, and Europe. Table 2 details the specific geographic constituencies of these samples, and Appendix A outlines archival sources and associated research institutions for crania provided. Appendix B provides exact measurements taken for each specimen. These samples broadly span the ecogeographic distribution of humans on Earth, ranging from polar tundra, temperate mid-latitudes, and equatorial tropics. The Equatorial African sample includes 17 individuals of known Kenyan or Liberian provenience, along with 33 individuals that lack exact provenience beyond a regional "West Africa" designation (Meigs, 1857; Renschler, 2007). The Arctic Circle sample is comprised of 75 Alaskan Iñupiat from Point Hope and Barrow, Alaska. The East Asian sample consists of 42 Mongolians and Buriats from northern Mongolia/Southern Siberia. The European sample is derived from as far north as Scandinavia to the more temperate Dalmatia region of Croatia. To increase sample size, the European sample also includes European-American crania housed in the Terry Collection (Smithsonian, Washington, D.C.). Previous studies (Chierci et al, 1973; Anton, 1989) have demonstrated that nasal morphology is highly stable between Europeans and European-Americans, permitting the reliable consolidation of these European-derived populations.

Only adult crania were utilized, which had been previously classified by the archivists of the crania based on either the eruption of third molars or fusion of the spheno-occipital synchondrosis (Buiktstra & Ubelaker, 1994). Selection was also based on presence of all anatomical features necessary for the collection of landmarks used to derive measurements on at least one side of the nasal cavity. This required individuals to exhibit an intact nasal septum, superior turbinate, and orbital lamina papyracea. For individuals possessing only one intact side, bilateral breadth measurements were calculated by doubling the unilateral value. Individuals with obvious craniofacial pathologies were also excluded, including those with abnormally (>2mm) pneumatized features within the airway, such as concha bullosa, Haller cells, and septal bulla (see Introduction).

Sex for the majority of crania is known from museum documentation. Although attempts were made to obtain samples with equal numbers of males and females, damage to delicate structures (e.g., turbinates, paper thin regions of the ethmoid) resulted in most samples exhibiting some degree of sex bias in order to maintain statistically reliable sample sizes. Moreover, sex is unknown for approximately 10% of the sample, most of which lack diagnostic features permitting reliable osteological sexing (Bastir et al., 2011; Holton et al., 2016; Schlager & Rudell, 2015). As it has previously been shown that indigenous females and males from the same geographical area share similar nasal morphologies (Corey et al., 1998; Franciscus, 1995), and that climate-mediated pressures similarly affects both sexes (Hall, 2005; Noback et al., 2011), all analyses in this study were conducted on combined sex samples.

Table 2. Overview of Specimens. Number of individuals per region with corresponding latitude by population and sex. See Appendix A for further details about sample origin.

Ecogeographic Region (♂,♀, Unknown)	**Population**	**Latitude**
Tropical, hot-wet	Kenya (n=12)	0.025°S
Equatorial Africa	Liberia (n=6)	6.5°N
n=50 (27, 14, 9)	West Africa (n=32)	2.5 °S - 16°N
Temperate	Buriat (n=23)	51.5°N
East Asia	Mongolia (n=19)	46.5 - 50°N
n=42 (19, 23)		
Temperate	Dalmatia (n=17)	45°N
Europe	Germany (n=5)	51 °N
n=48 (33, 13, 2)	Netherlands (n=1)	52 °N
	Scandinavia (n=8)	55 - 61°N
	United States (n=17)	N/A
Cold-dry	Pt. Hope (n=61)	68 °N
Arctic Circle	Barrow (n=14)	71 °N
n=75 (37, 32, 6)		

Measurements

Data were collected from CT images using 3D Slicer image processing software (version 4.10.2 r28257, Federov et al., 2019). Images were first transformed and volume rendered using Slicer modules and then aligned to the Frankfurt model to provide a consistent, biologically-relevant plane of reference for all crania. To initially assess whether SEB was an accurate proxy for FEB, three dimensional coordinates representing 18 nasal cavity landmarks (Figure 4; Table 3) were collected from the nasal cavity in 215 crania samples. These landmarks were chosen to best reflect major aspects of nasal cavity shape that affect the internal nasal fossa (Table 4). Some of these are well-established anthropological landmarks (Brauer, 1988; Buikstra & Ubelaker, 1994; Charles, 1930; Franciscus, 1995), whereas others were defined by this study to quantify particular aspects of the nasal anatomy.

Specifically, FEB was determined for the first time by this study; therefore, a methodology for obtaining the plane of section needed to be developed. FEB was demarcated as the distance from the left to right external ethmoidal walls at approximately 50% of the anterior nasal cavity coronal plane at landmarks #5-11 (Figure 4; Table 3, 4). This location significantly eliminated concerns of misclassifying EAC and MT from structures in the frontal recess (See Introduction: Variation in Nasal Anatomy). While the horizontal plane was used to ensure the most linear distance was taken between landmarks #1-4, 5-11, 13-15, and 16-18, obtaining the required anatomical measurements (e.g., intact biEAC, SM, SCM, and NS) for FEB determined the ultimate plane of section coronally over the other evaluated breadths. FEB was taken at the widest position of biEAC, SM, and SCM cumulatively, which was approximately halfway between the CG superiorly and by vomeronasal septum (VNS) inferiorly for most specimens.

To enhance measurement accuracy, landmarks were collected from the same coronal CT image slice whenever the relevant anatomy permitted. Linear measurements (in mm) were calculated from the landmarks using the Euclidean distance formula. Measurements were chosen to broadly sample the different functional components of the internal nose and nasal cavity, previously considered relevant to cold adaptation (Antón, 1989; Chierici et al., 1973; Churchill et al., 2004; Holton et al., 2013; Keck et al., 2000a; Maddux et al., 2011; Mlynski et al., 2001). SEB, FEB, and cavity breadth were taken individually and averaged between left and right sides. FEB was further broken down into functional airway space, including the SM and SCM breadths, and nonfunctional EAC breadth. The averages of both anatomical sides of these breadths were taken and doubled and were within +/- 0.1 mm of FEB. Cavity heights were described using midpoints between bilateral common meatal height (anatomically within the crista galli) and the most inferior nasal cavity points (approximately beneath the osteometric nasopinale). By combining the measurements of both passages, any problems caused by minimally deviated septa should be alleviated. To prevent interobserver error, all landmarking and subsequent measurement calculations were performed exclusively by the author.

Figure 4. Locations of landmarks on CT imaging.

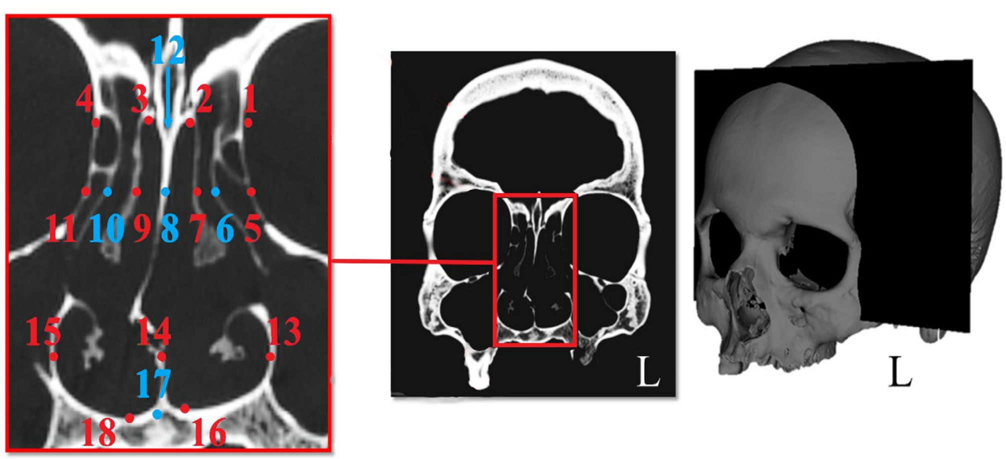

Visualized on 3D Slicer (Version 4.10.2 r2825, Federov et al., 2019). Frontal (coronal cross-section) view utilizing specimen #VL033 (see Appendix). Numbers correspond to landmarks in Table 3. Measurements elucidated in Table 4.

Statistical Analyses

The primary purpose of this study is to test whether 1) SEB is a reliable proxy for actual internal nasal airway dimensions, and 2) whether actual internal airway dimensions follow predicted ecogeographic patterns (i.e., narrower airways in colder environments and wider airways in in hotter environments). To evaluate the first question, linear regression was performed employing SEB as the independent (predictor) variable and the various measures of actual airway dimensions (e.g., FEB, EAC, airway) as dependent variables. To assess the second question, Kruskal-Wallis Analyses of Variance (ANOVA) were conducted to test for significant differences between the 4 regional groups. Dunn's post-hoc tests were subsequently performed to assess whether specific pairwise differences conform to morphological expectations. Non-parametric analyses were specifically conducted due to significant deviations from normality in some of the samples. Statistical significance for all analyses was assessed at $\alpha = 0.05$ and all statistical analyses were conducted in the NCSS software package (NCSS 11, 2016).

Table 3. Definitions of 18 nasal cavity landmarks representing internal airway features used in this study. Left and right anatomy distinguished by first, second value respectively.

Landmark	Osteometric Name	Description
1, 4	-	Frontoethmoidal suture from external margin
2, 3	-	Common meatal height
5, 11	-	External ethmoidal wall at level of widest superior meatal and superior common meatal breadths
6, 10	-	Internal ethmoidal wall at level of widest superior meatal and superior common meatal breadths
7, 9	-	Supreme turbinate
8	PPE	Perpendicular plate of ethmoid bone: superior nasal septum midpoint between supreme turbinates
12	CG	Crista galli: superior midpoint between common meatal heights
13, 15	Alare	Lateralmost margin on nasal aperture of transverse plane
14	VNS	Vomeronasal septum: inferior nasal septum midpoint between alares
16, 18	Nasale	Inferiormost margin on nasal aperture
17	Nasospinale	Inferiormost midpoint between nasals

Table 4. Definitions of linear coronal skeletal measurements used in this study. Anatomical left and right landmarks distinguished by first, second value respectively. In specimens with missing inferior nasal septum, nasal breadth did not utilize VNS (#14), therefore could not produce average between left and right.

Measurement	**Definition**
Superior Ethmoidal Breadth (SEB)	Maximum distance from right to left frontoethmoidal sutures (1-4)
L/R Half of SEB	Distance from left and right frontoethmoidal sutures to CG, used for averaging SEB values (1-2,12;3-4,12)
Functional Ethmoidal Breadth (FEB)	Maximum distance from left to right external ethmoidal walls at level of widest SM and SCM (5-11)
L/R Half of FEB	Averaged distance from left and right external ethmoidal walls to PPE (5-8, 8-11)
L/R Ethmoidal Aircell (EAC) Breadth	Averaged distance across left and right ethmoidal aircells (5-6, 10-11)
L/R Superior Meatus (SM) Breadth	Averaged distance across left and right superior meatuses (6-7, 9-10)
L/R Superior Common Meatus (SCM) Breadth	Averaged distance across left and right superior common meatuses (7-8, 8-9)
Nasal Breadth (NB)	Distance between the anterior edges of nasal aperture at its widest point (13-15)
Nasal Height (NH)	Distance of CG to the nasospinale (12,17)
L/R NH	Maximum vertical distance of left and right common meatal height to respective nasale (2,16;4,18)

RESULTS

Descriptive Variation in Internal Nasal Cavity Size

The results confirm that the position of SEB is consistently above the functional airways (Figures 5 and 6), superior of the roof of the internal nasal cavity and the horizontal plate the ethmoid bone, and typically narrower than FEB in both median and mean across all populations (Figure 5, Table 5). In accordance with my second hypothesis, Asians and Europeans exhibited similar SEB and FEB values, as would be expected from similar ecogeographic regions and latitudes. The median, mean, and standard deviation for each group are provided in Table 5. This study's SEB measurements are larger on average in the African sample and smallest in the Arctic sample also expected from hypothesis #2. FEB as a whole follows this pattern. However, when broken down into airway versus air cells, the African sample's airway is not the largest and the Arctic air cells are not the smallest. The Asian sample has the largest airway and the European the smallest air cells, which was not anticipated by their more intermediate SEB and FEB values. Still, in three-fourths (SEB, FEB, and EAC) of the evaluated breadths, the African sample exhibits the widest values and the Arctic sample the narrowest. The exceptions, however, may provide insight into how specific aspects of anatomy contribute to variation in superior nasal airway morphology.

Table 5. Descriptive Statistics of Linear Measurements Samples by Population. Values in red deviate from hypothesized results.

	Median	Mean	Standard Deviation
SEB			
Africa	28.3	27.9	2.8
Arctic	22.9	23.1	2.0
Asia	25.8	25.7	2.3
Europe	25.4	25.5	2.2
FEB			
Africa	29.4	29.1	3.1
Arctic	24.8	24.8	2.7
Asia	27.0	26.6	2.8
Europe	25.8	25.5	2.4
Airway			
Africa	13.3	13.3	2.0
Arctic	11.6	12.1	2.3
Asia	13.6	14.0	2.6
Europe	13.0	13.0	2.1
biEAC			
Africa	15.2	15.8	3.8
Arctic	12.3	12.7	3.2
Asia	12.4	12.6	3.3
Europe	12.2	12.5	2.7

Figure 5. Stacked bar chart displaying the scaling relationship between FEB, its components biEAC and airway, and SEB.

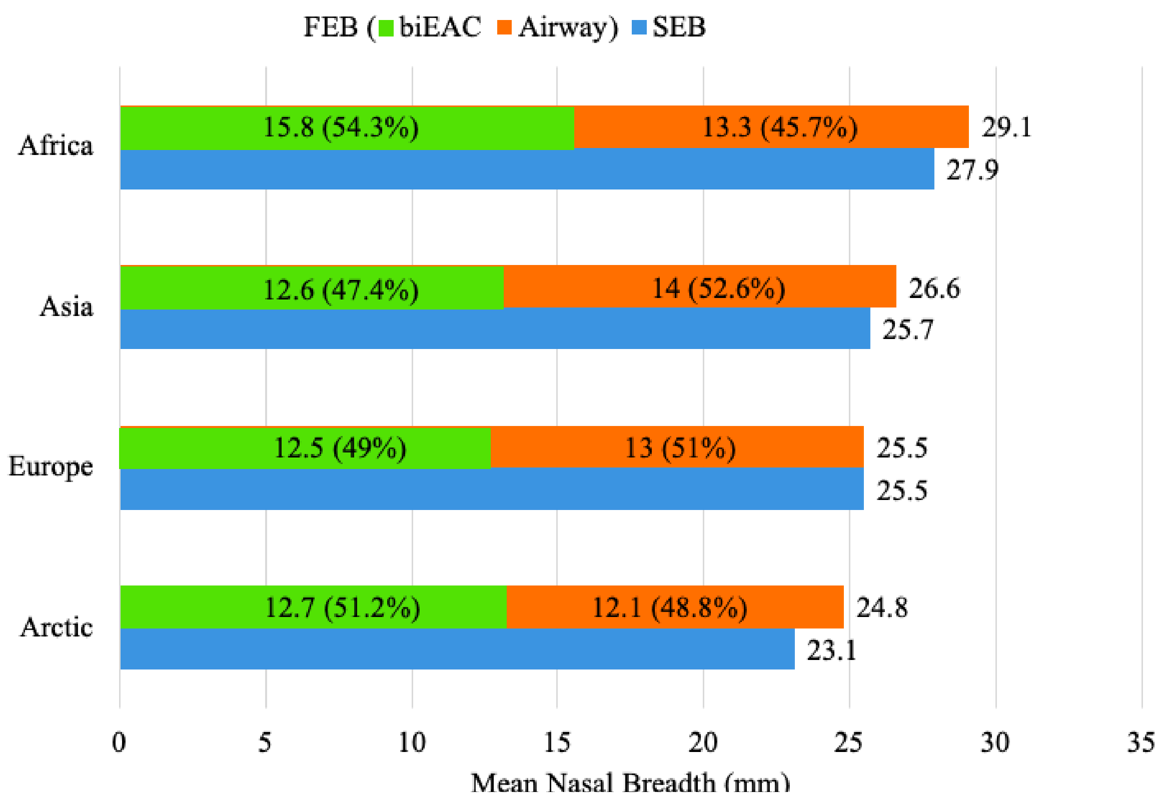

Figure 6. Coronal CT scan images of individuals with representative morphologies (most similar to calculated median SEB and FEB) for the evaluated populations.

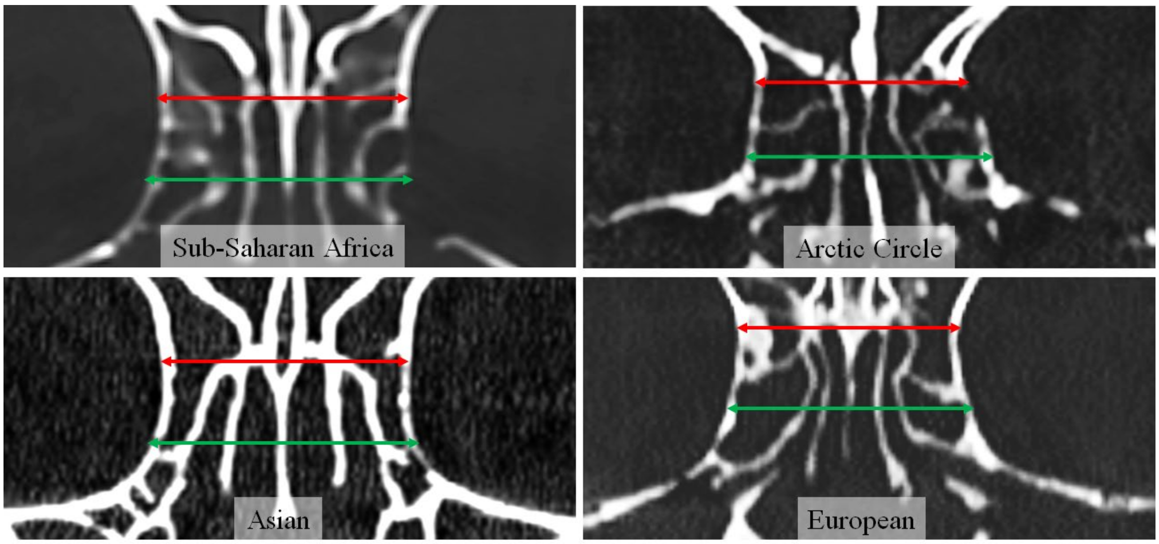

Images taken at 50% of anteroposterior plane of common and superior meatal breadth insertions. Specimen catalogue (see Appendices A,B): African #MOR0646, Arctic #001199, Asian # P278709, European #TC651. SEB is approximated in red and FEB in green on images for enhancing visualization and not reflective of exact measurements taken.

Linear Regression

Detailed results of regression analyses between SEB and the evaluated variables are presented in Table 6 and Figure 7. Bivariate regression indicates statistically significant relationships between SEB and each of the predicted variables, which was performed to confirm my first hypothesis. However, SEB only permits predication of FEB ($R^2 = 0.6591$) with any degree of accuracy, with SEB representing a relatively poor predictor variable for biEAC ($R^2 = 0.3370$, $p<.0001$) and especially airway ($R^2 = 0.0582$, $p<.0004$) representing poor predictor variables. Overall, SEB was highly correlated to the ethmoidal breadth taken at the functional level of the upper airways (i.e., functional airway breadth [FEB]) but did not include the superior airway structures, SM and SCM, and non-airway spaces, EAC.

Table 6. Linear regression results for average SEB on average FEB, airway, and biEAC measures across all samples.

	R	R^2	Slope	95% CI	p-Value
FEB	0.8119	0. 6591	0.8841	0.7982- 0.9700	**<0.0001**
Airway	0.2412	0.0582	0.1901	0.0868- 0.2934	**<0.0004**
biEAC	0.5805	0.3370	0.6934	0.5621-0.8248	**<0.0001**

Figure 7. Scatter plots of results from linear regression.

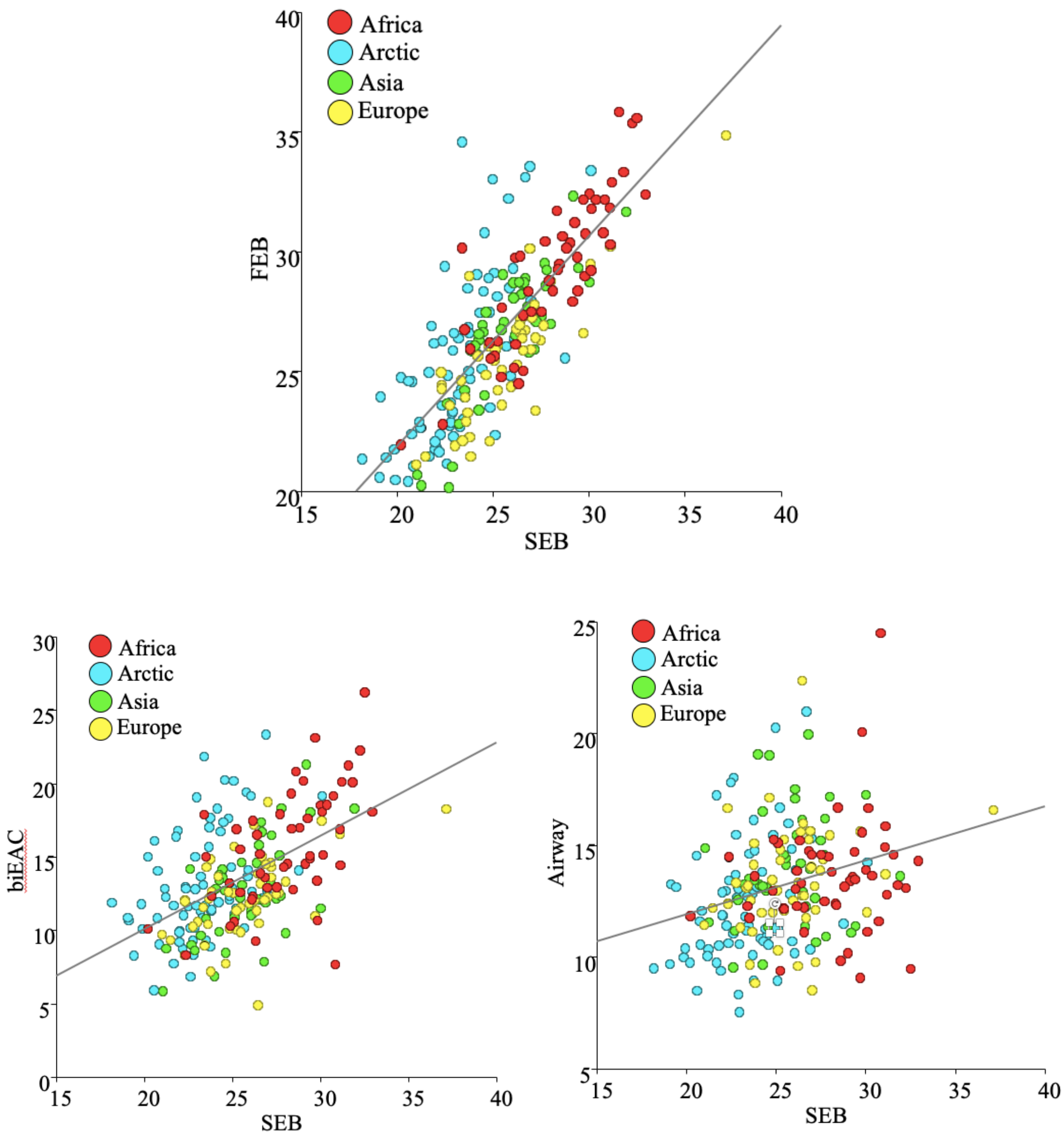

Average SEB values versus average FEB, airway, and biEAC values across all samples.

Kruskal-Wallis Tests

Results of Kruskal–Wallis tests conducted to investigate the signficance of the differences expected from the second hypothesis on average SEB, FEB, airway, and biethmoidal air cell values for human population samples in 4 different regions reveal significant differences among the four climatic groups for SEB (χ^2 = 82.1991, p<.0001), FEB (χ^2 = 54.2055.3, p<.0001), airway (χ^2 = 19.0295, p<.0001), and biEAC (χ^2 = 27.6673, p<.0001) Table 7 details the between-group variation of the t-tests utilizing Dunn's post hoc tests, and Figure 8 show box plots of the four examined variables. For SEB, Dunn's post-hoc results indicate that the African and Arctic samples are significantly different from all other samples, whereas the Asian and European samples are not significantly different from each other. For FEB, the African sample is again significantly different from all other samples, while the Arctic sample is only significantly different from the African and Asians samples. The Asian and European samples are again not significantly different from each other. For Airway, the Arctic sample is significantly different from all other groups, with no significant pair-wise differences between the African, Asian, or European samples. Conversely, for biEAC, the African sample is significantly different from all other groups, with no pairwise differences between the other three groups Cumulatively, these results supported FEB and SEB as a whole to be significant indicators for the African population, but did not indicate that all populations indigenous to colder-drier climates will exhibit narrower superior nasal airway (SCM and SM) dimensions compared to those from warmer-wetter environments.

Table 7. Results of Kruskal-Wallis Multiple-Comparison (Dunn's) Z-Value Test. Medians significantly different (z-value > 1.9600) indicated in Bold. Medians significantly different following Bonferonni correction (z-value > 2.6383) are also italicized.

	Africa	Arctic	Asian	European
SEB				
Africa	-			
Arctic	***8.8462***	-		
Asian	***3.1544***	***4.9544***	-	
European	***3.6229***	***4.7771***	0.3400	-
FEB				
Africa	-			
Arctic	***7.0724***	-		
Asian	***3.1343***	***3.2959***	-	
European	***5.2544***	1.2414	1.9203	-
Airway				
Africa	-			
Arctic	***3.1497***	-		
Asian	0.8893	***3.9496***	-	
European	0.6495	**2.4010**	1.5021	-
biEAC				
Africa	-			
Arctic	***4.6353***	-		
Asian	***3.9369***	0.1155	-	
European	***4.3189***	0.1431	0.2305	-

Figure 8. Box plots of each examined breadth across the four regional samples.

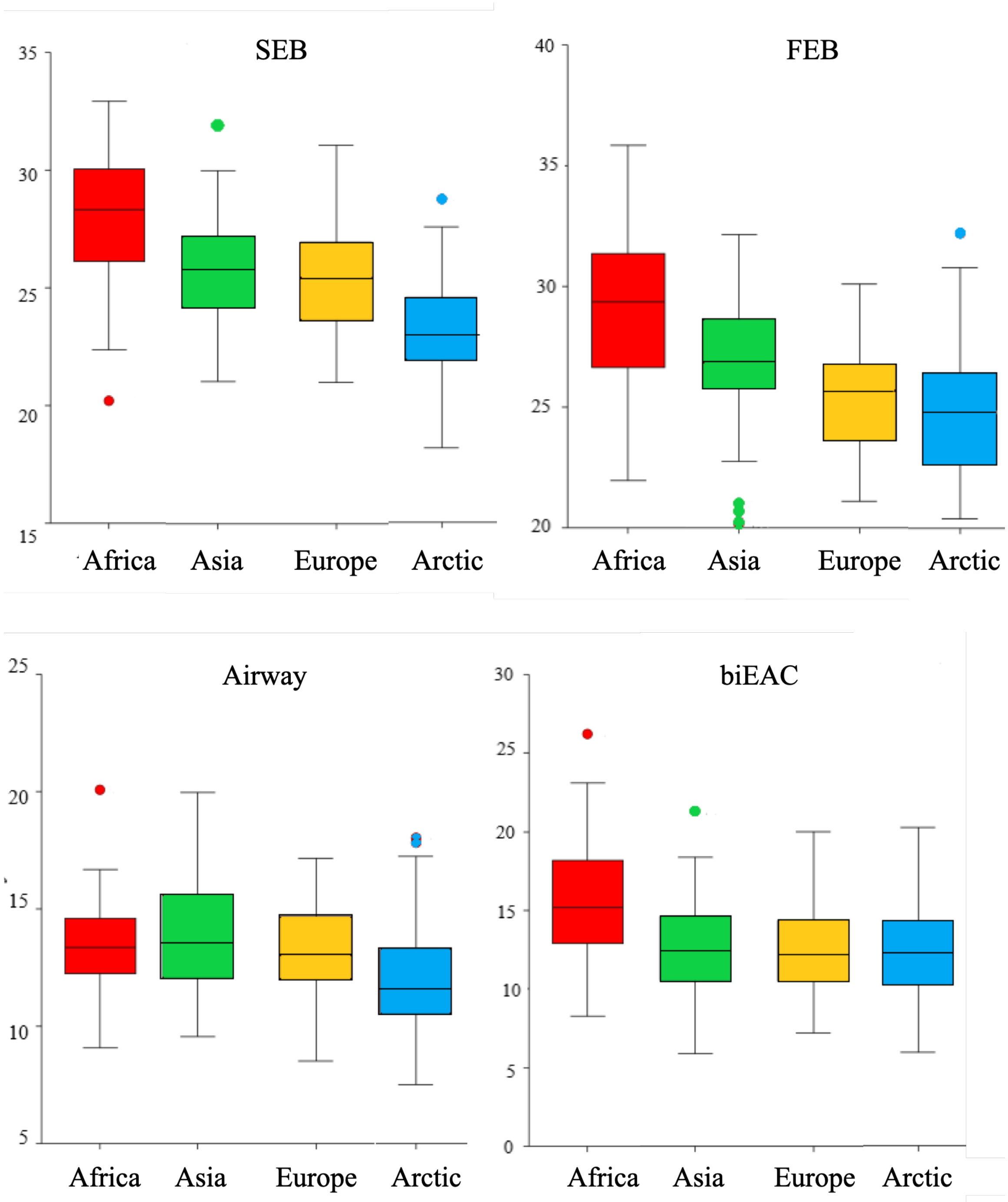

DISCUSSION

This study aimed to describe how internal nasal morphologies vary among peoples from the very cold-dry, temperate, and hot-humid regions, and to assess the extent to which SEB represents a reliable proxy for internal airway dimensions. To the best of my knowledge, this study is the first to test associations between SEB and the functional airways of the human nose and to assess geographically-patterned variation in superior nasal airway morphology across human populations from climatically diverse regions. In addition, this study developed a novel methodological approach for accurately quantifying the complex nasal morphology of the superior nasal airways, an anatomical region that has ostensibly only been investigated through endoscopic studies. Cumulatively, these results support use of SEB as proxy for upper nasal airway breadth and provides potential functional rationale for correlation between SEB and climatic variables.

While this study found strong evidence to support associations between SEB and the internal dimensions of the ethmoid at the level of the functional airways (i.e., FEB), results indicate weaker associations between SEB and the separate airway and air-cells components which comprise FEB. Accordingly, this study provides somewhat equivocal support for the hypothesis that SEB represents a reliable proxy for internal airway dimensions. Indeed, while SEB clearly represents a reliable and readily accessible way of assessing overall breadth of the internal ethmoid when imaging data is not available, this study suggests the SEB is only weakly associated with dimensions of functional airways (i.e., common and superior meatus breadths). While this result may initially appear to undermine the use of SEB as a proxy for internal airway dimensions, this result may also be attributable to the considerable variation in superior nasal passage anatomy. In this study, measurements of airway breadth were assessed more superiorly (approximately 5 cm) within the ethmoidal complex than previous studies evaluating CM breadth (Maddux et al., 2017; Marks et al., 2019; Noback et al., 2011; Yokley, 2009). This was the first time to my knowledge that a study concurrently accounted for both SCM and SM breadth at the same functional level while taking into account recent endoscopic advances in anatomical knowledge (Psaltis & Wormald, 2019). In many individuals, determination of the relative supero-inferior location of FEB (and subsequently CM, SM, and EAC breadths) was complicated by unusual extrasinusal pneumatizations, such as concha bullosa (Cobzeanu et al., 2014; Gibelli et al., 2018; Maroldi et al., 2005; Nicoleta et al., 2015), and the intactness of crania that are several centuries old. Given the complexity of this area of the nasal passages, additional research is needed to further evaluate breadth dynamics at multiple vertical levels throughout the upper nasal passages. In particular, 3D geometric morphometric analyses employing type 3 semi-landmarks may provide valuable information regarding shape variation in superior nasal airway morphology. Such analyses may provide more nuanced understanding of how SEB relates to functional airway dimensions.

Across the majority of examined variables, the African sample demonstrated greatest superior nasal breadths and the Arctic sample the narrowest breadths, with Asian and European samples typically exhibiting intermediate morphology. These results generally support the second hypothesis, which posited that populations adapted to colder-drier climates would exhibit narrower superior nasal airway dimensions compared to those from warmer-wetter environments. These results thus extend the widely accepted idea (Bastir et al., 2011; Butaric, 2015; Butaric & Klocke, 2018; Franciscus, 1995; Fukase et al., 2016; Holton et al., 2013; Maddux et al., 2017; Noback et al., 2011; Yokley, 2009) that internal nasal breadth dimensions should inversely scale with increasing latitude (i.e., wider at lower latitudes), and thus, scale positively with climatic variables such as temperature and absolute humidity (i.e., wider in hotter, wetter environments), to the superior aspects of the nasal cavity. Still, a number of counterintuitive results were also revealed during this study which require further examination. Below, the results of this study are discussed in more detail in relation to each of the four geographic samples included in this study.

Equatorial Africa

It was expected that all breadth values would be largest in the African sample, and this was supported by the African sample exhibiting the widest average FEB, SEB, and EAC values in the study. Previous studies have suggested that the relatively small turbinates of Equatorial Africans, combined with larger common meatus and inferior airway dimensions, would produce a larger cross-sectional area adapted for maximizing heat and moisture losses during expiration (Marks et al., 2019). Yet, the superior nasal airways of the Equatorial African sample in our study (i.e., combined CM and SM breadths) were only significantly wider than those seen in the Arctic sample. Moreover, the average airway value for the African sample was actually narrower than that seen in the East Asian sample, both in terms of absolute dimensions (13.3 mm < 14 mm) and relative proportion of total FEB (45.7% < 52.6%). Interestingly, rather than being attributable to the widest airway dimensions, the wide FEB values seen in the African sample appear predominantly attributable to the sample possessing exceedingly wide biEAC values. In fact, not only did the African sample exhibit the absolutely widest biEAC dimensions, these wide biEaC values typically constituted more than half (54.3%) of the total FEB dimension. While this study largely assumes EAC is a non-functional airway measurements (i.e., not an area through which the respiratory airstream flows), the EACs do have important immune functions (Maroldi et al., 2005; Tos, 1982) and also contribute to the overall structural architecture of the nasal cavity (Butaric, 2019; Inthvahong et al., 2007; Lang, 1989). Previous studies have argued that climate-mediated morphology adaption in the morphology of the paranasal sinuses contributes to respiratory health (Eccles, 2002; Uliyanov, 1998), and the disproportionately large EACs in the African sample may reflect selection related to pathogen filtration rather than heat/moisture transfer. Alternatively, as the EACs represent a structural intermediary between the superior nasal airways and the ocular orbit, the wide EACs seen in our African sample could relate to overall patterns of integration/modularity between the nasal complex and the rest of the face. Indeed, a number of studies (Holton et al., 2013; Butaric & Maddux, 2016; Maddux & Butaric, 2017) have argued the maxillary sinuses represent "zones of accommodation" within the midface, effectively disconnecting the lower nasal cavity from other midfacial structures such as the dentition, masticatory musculature, and inferior orbit. It thus appears plausible that the EACs could represent similar “accommodative” structures, permitting some degree of independence between the superior nasal cavity and orbits during growth and development.

The Arctic Circle

In contrast to the African sample, it was expected that the breadth values would, on average, be smallest in the Arctic population. The Arctic sample generally conformed to these expectations, demonstrating significantly narrower SEB, FEB, and airway values compared to all other evaluated populations. The narrow nasal airways of the Arctic sample also represented a smaller (48%) proportion of total FEB compared to both Europe (51%) and Asia (52.6%) from more temperate climates. As a consequence, it appears likely that a smaller amount of respired air would pass through the SM and SCM relative to the amount of mucosa (i.e., greater SA/V ratio) in the Arctic sample compared to the other samples in the study. This supports prior hypotheses that increased air-to-mucosa contact in cold-dry populations enhances the air conditioning capacity of the nasal passage (Franciscus & Long, 1991; Maddux et al., 2017; Naftali et al., 2005; Yokley, 2009). Colder climate populations characterized by smaller internal superior dimensions have ultimately been linked to aspects of airflow dynamics and general respiratory health (Uliyanov, 1998), which may be influenced by the increased volume of the nasal cavity and immune cells due to a proportion of EAC, and constitutes the majority (51.2%) of overall FEB. It has been hypothesized by other studies (Elad et al., 1993; Marks et al., 2019, Uliyanov, 1998) that a greater percentage of the total respiratory volume among cold-dry adapted individuals is redirected superiorly toward the upper nasal cavity (e.g., middle, superior, and upper common meatuses) for enhanced air-conditioning compared to equatorial counterparts. The results of this study suggest that redirection of the respiratory airstream to the superior nasal passages likely forces respired air into exceedingly narrow channels, maximizing contact between the air and the surrounding mucosa.

East Asia

Deriving from a temperate climate, the East Asian sample comprised of Mongolian and Buriat crania was expected to display relatively intermediate morphology compared to both the Arctic and African samples. It was also expected that the Asian sample would be morphologically similar to the European sample, as both samples derived from similar latitudes and temperature. While these expectations were generally met for SEB and FEB, the Asian sample's airway and biEAC values both deviated from morphological expectations. Undoubtedly the most interesting result was the Asian sample exhibiting absolutely wider airway dimensions (14 mm) than the African sample (13.3 mm). The fact that this study focused exclusively on breath dimensions, rather than relative breadth/height dynamics, may represent one potential explanation. In this study, no attempt to quantify the height of the superior nasal airways was undertaken as there is no clear boundary delineating between "inferior" and "superior" aspects of the nasal passages. Still, previous research on the nasal index (Franciscus & Long, 1991; Leong & Eccles, 2009; Thomson, 1913; Thomson & Buxton, 1923; Wolpoff, 1968) has shown that both nasal breadth and height dimensions are associated with climatic variables. As a consequence, it also highlights the considerable variability in the airway vs EAC contribution to overall FEB. For example, while in the African sample the EACs comprised more than half (54.3%) of total ethmoidal breadth, the airway was found to constitute the majority (52.6%) of total breadth in the Asian sample. Although it remains unclear whether these differences have functional consequences, it is apparent that there is not a consistent pattern of airway-to-EAC proportionality across humans. This result highlights the possibility that different selective pressures may be acting on the airways and EACs (e.g., air-conditioning vs immunological), or minimally, that selective pressures on airway dimensions have had little evolutionary impact on EAC morphology.

Europe

Like the East Asian sample, the European sample was predicted to exhibit intermediate breadth values compared to both the African and Arctic samples. For the most part, the European sample did in fact display intermediate breadth values, exhibiting SEB, FEB, and airway values falling between those exhibited by the two climatic extreme samples. However, while displaying intermediate mean values, it should be noted that the European sample was only significantly different from both the African and Arctic samples for SEB. Perhaps most surprisingly, the mean airway breadths seen in the European sample (13 mm) is generally comparable to that seen in the African sample (13.3 mm). Thus, the smaller overall FEB value in the European sample compared to Africans appears more attributable to the European sample possessing significantly narrower EACs rather than narrower airways. Conversely, the average airway dimension of the European sample was found to be significantly wider than that of the Arctic sample. This result appears generally consistent with the theoretical expectation that higher demands for inspiratory air-conditioning in the Arctic resulted in evolutionary selection for significantly narrower superior nasal passages compared to that need to effectively condition air in temperate climates. Still, the lack of significant differences in airway breadths between the European and African samples remains somewhat perplexing. While, again, this result could potentially relate to the relative breadth vs. height dynamics discussed previously, the similar airway breadths present in the European and African samples ignores the possibility that these breadth dimensions could differ considerably relative to vertical dimensions of the SCM and/or SM. Thus, additional research is needed to assess superior nasal airway heights, as, if the European sample possesses taller vertical dimensions, this morphology would translate to higher SA/V ratios than in the African sample, and thus conform to overall functional predictions for enhanced air-conditioning capabilities in temperate climates compared to tropical environments.

Clinical Considerations

While investigations of ecogeographic variation in nasal morphology has a long history within the anthropological literature, the clinical literature -- focused extensively on internal nasal physiology-- has generally not applied information regarding geographically-patterned variation into clinical-focused investigations. Not only would this anatomical knowledge contribute to improving surgical procedures, it may also provide insights to clinical modeling for the effects of temperature and humidity that occur within the respiratory tract. As mentioned previously, septal deviation is a common cause of obstruction, which, in addition to turbinate hypertrophy, is important because nearly half of the airflow is in the middle portion of the airway (Doorly et al., 2008, Uliyanov, 1998). Turbinates adjacent to septal damage or concha bullosa may exhibit hypertrophy secondary to nasal airway turbulence, causing further airway resistance (Nicoleta et al., 2015). As long as this resistance contributes to turbulent flow without significant obstruction, there could be an increased or equivalent functionality of recapturing heat and humidity during expiration with minor septal deviation or pneumatization.

The nasal mucosa is highly adapted to meet environmental challenges, so it is logical that the upper airway is proficient in responding to inflammation. Both allergic and non-allergic rhinopathies (disorders with seasonal and perennial nasal congestion, rhinorrhea, and/or sneezing) are affected by climate through a variety of mechanisms and treated through even more means, ranging from medical to surgical (Eccles, 2002; Marquez, 2008). An acute example is provided through individuals who, within minutes of exposure to cold air, have similar symptoms that dissipate soon after exposure is terminated. Several studies have also examined respiratory diseases, such as asthma, to be associated with local changes in temperature (Eccles, 2002; Havenith, 2005; Marquez, 2008). The relative effects of an individual's airway size, alongside the EAC's immunological functions, may contribute to the convection of water vapor on the mucosa during inspiration and condensation during expiration and evaporation due to difference in temperature or humidity in a given climate.

Rhinoplasty, the surgical procedure for changing the shape of the nose while preserving or enhancing the nasal airway, is one of the most pervasively performed cosmetic procedures in the United States (Leong & Eccles, 2009). If remodeling is to be considered a therapeutic target, understanding the variation and functional breadth of the anatomy provides a chance to reverse or even prevent disease. Actively targeting the relevant nasal anatomy at an early stage might be most effective in reducing the consequences of invasive procedures. Advancing patient care should continue to drive the need for accurate anatomical descriptions of the nasal airway. Since this is an area of the crania that has involved persistent perplexity and ambiguity in nomenclature (Marquez, 2008; Psaltis & Wormald, 2019), more accurate imaging techniques and greater collaboration between disciplines, such as anthropologists, radiologists, and otolaryngologists, with morphometrics, MR, and PET imaging will allow significant progression in these findings.

Conclusions

This study investigated whether variation in superior nasal cavity (i.e., ethmoidal) breadth dimensions across human populations has been driven by regional differences in climate. SEB was found to be highly correlated with FEB across human population samples, validating the common use of SEB as an externally measured proxy for the internal breadth of the ethmoid at the level of the airway. However, results also indicate that the association between SEB and internal airway (common and superior meatuses) breadths is relatively weak, suggesting the assumption that SEB accurately reflects superior nasal passage dimensions must be viewed with caution. Still, the results of this study generally support claims that local adaptation to climate likely played an important role in the evolution of nasal shape across human populations. Indeed, the nasal morphologies seen in each of the four geographic samples included in this study generally conforms to theoretical expectations for climatic adaptation, with individuals indigenous to cold-dry Arctic environments typically exhibiting the narrowest superior nasal cavity breadths, individuals from hot-humid Equatorial Africa usually exhibiting the widest breadths, and individuals from the temperate climates of Europe and East Asia exhibiting relatively intermediate breadth dimensions.

While generally supporting previous assertions that climate has played a role in shaping superior nasal cavity morphology, some of the more equivocal results highlight the need for further research into the morphology of superior nasal cavity anatomy. In particular, as this study focused exclusively on breadth dimensions, considerably more research is required to assess the height and length dynamics of the superior nasal cavity. Moreover, as noted earlier, this study assessed breadth dimensions at a single vertical plane. Thus, information regarding the variability of breath dimensions, not only across different supero-infererior levels of the nasal cavity, but also along the antero-posterior length of the nasal cavity, would likely provide valuable information regarding respiratory airflow patterns and air-conditioning processes. Information regarding SM and SCM variability is still necessary to more fully understand the ecogeographic patterning of the nasal complex as a whole, and there still remain many issues to be addressed regarding nasal morphofunctional significance. Nevertheless, through building upon and establishing new landmarks consistent across the intricate internal airways of both *in* and *ex vivo* crania, these methodological discoveries will be valuable for further investigation into what factors impact nasal morphology. Accordingly, while accurately assessing the complex anatomy of the superior nasal cavity represents a daunting methodological challenge, the potential benefits for better understanding nasal form and function warrant additional investigation. In particular, while the populations from two climatic extremes (cold-dry and hot-humid) contextualized the differences in superior airway dimensions, future investigations into airway shape among humans in more temperate environments will be exceedingly informative for explaining variable meatal breadths as it relates to ethmoidal air cells.

APPENDIX A: SKULL SOURCES

Equatorial African Ancestry Specimens

West African skulls scanned by Drs. Janet Monge and Tom Schoenemann of the Open Resource Scan Archive at University of Pennsylvania (Philadelphia, P.A.) or by Dr. Lauren Butaric and stored in the National Museum of Natural History (Washington, D.C.). The Cuban population were first generation immigrants from West Africa, and samples lack exact regional provenience. East African skulls scanned by Dr. David Hunt and stored in the Smithsonian National Museum of Natural History (New York City, N.Y.).

Table 8. Equatorial African Collection, Credited Sources, and Archivists

ID	SEX	REGION	POPULATION	MUSEUM	SCANNER
MOR0645	Male	West Africa	Liberia- Graboo	Penn	ORSA
MOR0646	Female	West Africa	Liberia- Bassa	Penn	ORSA
MOR0647	Male	West Africa	Liberia- Bassa	Penn	ORSA
MOR0914	Female	West Africa	Cuba	Penn	ORSA
MOR0915	Male	West Africa	Cuba	Penn	ORSA
MOR0917	Male	West Africa	Cuba	Penn	ORSA
MOR0920	Unknown	West Africa	Cuba	Penn	ORSA
MOR0923	Unknown	West Africa	Cuba	Penn	ORSA
MOR0924	Unknown	West Africa	Cuba	Penn	ORSA
MOR0925	Unknown	West Africa	Cuba	Penn	ORSA
MOR0927	Unknown	West Africa	Cuba	Penn	ORSA
MOR0963	Male	West Africa	Cuba	Penn	ORSA
MOR0964	Male	West Africa	Cuba	Penn	ORSA
MOR0968	Male	West Africa	Cuba	Penn	ORSA
MOR0971	Male	West Africa	Cuba	Penn	ORSA
MOR0974	Male	West Africa	Cuba	Penn	ORSA
MOR0975	Male	West Africa	Cuba	Penn	ORSA
MOR0976	Unknown	West Africa	Cuba	Penn	ORSA
MOR0978	Male	West Africa	Cuba	Penn	ORSA
MOR0993	Female	West Africa	Cuba	Penn	ORSA
MOR0994	Unknown	West Africa	Cuba	Penn	ORSA
MOR1100	Male	West Africa	Liberia-Eboe	Penn	ORSA

MOR1102	Female	West Africa	Liberia-Eboe	Penn	ORSA
P049446	Female	West Africa	Liberia	NMNH	Butaric
P244050	Male	West Africa	Senegal	NMNH	Butaric
P244052	Male	West Africa	Ghana	NMNH	Butaric
P244055	Unknown	West Africa	Ghana	NMNH	Butaric
P244057	Male	West Africa	Ghana	NMNH	Butaric
P276088	Male	West Africa	Gabon	NMNH	Butaric
P276090	Female	West Africa	Gabon	NMNH	Butaric
P276092	Female	West Africa	Gabon	NMNH	Butaric
P276093	Female	West Africa	Gabon	NMNH	Butaric
P276348	Male	West Africa	Cameroon	NMNH	Butaric
P302767	Male	West Africa	French Congo	NMNH	Butaric
P323695	Male	West Africa	Congo Republic	NMNH	Butaric
P381071	Male	West Africa	Gabon	NMNH	Butaric
P381074	Unknown	West Africa	Gabon	NMNH	Butaric
P381076	Male	West Africa	Gabon	NMNH	Butaric
P257540	Male	East Africa	Kenya	NMNH	Hunt
P257548	Female	East Africa	Kenya	NMNH	Hunt
P257549	Female	East Africa	Kenya	NMNH	Hunt
P257584	Male	East Africa	Kenya	NMNH	Hunt
P257587	Female	East Africa	Kenya	NMNH	Hunt
P257588	Male	East Africa	Kenya	NMNH	Hunt
P257591	Male	East Africa	Kenya	NMNH	Hunt
P257594	Male	East Africa	Kenya	NMNH	Hunt
P257599	Female	East Africa	Kenya	NMNH	Hunt
P273199	Female	East Africa	Kenya	NMNH	Hunt
P273205	Female	East Africa	Kenya	NMNH	Hunt
P273207	Male	East Africa	Kenya	NMNH	Hunt

Arctic Circle Ancestry Specimens

Pt. Hope and Barrow, Alaska skulls scanned by Giselle Garcia and Dr. David Hunt and stored in either the American or National Museum of Natural History (New York City and D.C.), respectively.

Table 9. The Arctic Circle Collection, Credited Sources, and Archivists

ID	SEX	REGION	POPULATION	MUSEUM	SCANNER
99187	Male	Arctic	Pt. Hope- Tigara	AMNH	Garcia
991102	Female	Arctic	Pt. Hope- Tigara	AMNH	Garcia
991103	Male	Arctic	Pt. Hope- Tigara	AMNH	Garcia
991166	Male	Arctic	Pt. Hope- Tigara	AMNH	Garcia
991168	Female	Arctic	Pt. Hope- Tigara	AMNH	Garcia
991181	Male	Arctic	Pt. Hope- Tigara	AMNH	Garcia
991194	Male	Arctic	Pt. Hope- Tigara	AMNH	Garcia
991197	Female	Arctic	Pt. Hope- Tigara	AMNH	Garcia
991199	Female	Arctic	Pt. Hope- Tigara	AMNH	Garcia
991224	Male	Arctic	Pt. Hope- Tigara	AMNH	Garcia
991234	Female	Arctic	Pt. Hope- Tigara	AMNH	Garcia
991235	Male	Arctic	Pt. Hope- Tigara	AMNH	Garcia
991237	Male	Arctic	Pt. Hope- Tigara	AMNH	Garcia
991240	Female	Arctic	Pt. Hope- Tigara	AMNH	Garcia
991248	Female	Arctic	Pt. Hope- Tigara	AMNH	Garcia
991250	Male	Arctic	Pt. Hope- Tigara	AMNH	Garcia
991252	Male	Arctic	Pt. Hope- Tigara	AMNH	Garcia
991257	Female	Arctic	Pt. Hope- Tigara	AMNH	Garcia
991260	Female	Arctic	Pt. Hope- Tigara	AMNH	Garcia
991262	Female	Arctic	Pt. Hope- Tigara	AMNH	Garcia
991268	Female	Arctic	Pt. Hope- Tigara	AMNH	Garcia
991276	Female	Arctic	Pt. Hope- Tigara	AMNH	Garcia
991277	Male	Arctic	Pt. Hope- Tigara	AMNH	Garcia
991278	Male	Arctic	Pt. Hope- Tigara	AMNH	Garcia
991282	Female	Arctic	Pt. Hope- Tigara	AMNH	Garcia
991296	Male	Arctic	Pt. Hope- Tigara	AMNH	Garcia
991324	Unknown	Arctic	Pt. Hope- Tigara	AMNH	Garcia
991330	Female	Arctic	Pt. Hope- Tigara	AMNH	Garcia
991332	Female	Arctic	Pt. Hope- Tigara	AMNH	Garcia
991334	Female	Arctic	Pt. Hope- Tigara	AMNH	Garcia
991335	Female	Arctic	Pt. Hope- Tigara	AMNH	Garcia
991336	Male	Arctic	Pt. Hope- Tigara	AMNH	Garcia
991339	Male	Arctic	Pt. Hope- Tigara	AMNH	Garcia
991340	Male	Arctic	Pt. Hope- Tigara	AMNH	Garcia
991345	Female	Arctic	Pt. Hope- Tigara	AMNH	Garcia
991346	Male	Arctic	Pt. Hope- Tigara	AMNH	Garcia
991355	Female	Arctic	Pt. Hope- Tigara	AMNH	Garcia
991357	Male	Arctic	Pt. Hope- Tigara	AMNH	Garcia
991362	Female	Arctic	Pt. Hope- Tigara	AMNH	Garcia
991364	Male	Arctic	Pt. Hope- Tigara	AMNH	Garcia

991373	Male	Arctic	Pt. Hope- Tigara	AMNH	Garcia
991459	Female	Arctic	Pt. Hope-Tigara	AMNH	Garcia
991510	Female	Arctic	Pt. Hope- Tigara	AMNH	Garcia
991511	Male	Arctic	Pt. Hope- Tigara	AMNH	Garcia
991513	Female	Arctic	Pt. Hope- Tigara	AMNH	Garcia
991515	Male	Arctic	Pt. Hope- Tigara	AMNH	Garcia
991519	Unknown	Arctic	Pt. Hope- Tigara	AMNH	Garcia
991520	Male	Arctic	Pt. Hope- Tigara	AMNH	Garcia
991524	Female	Arctic	Pt. Hope- Tigara	AMNH	Garcia
991525	Male	Arctic	Pt. Hope- Tigara	AMNH	Garcia
991526	Female	Arctic	Pt. Hope- Tigara	AMNH	Garcia
991542	Male	Arctic	Pt. Hope- Tigara	AMNH	Garcia
991546	Female	Arctic	Pt. Hope- Tigara	AMNH	Garcia
991549	Male	Arctic	Pt. Hope- Tigara	AMNH	Garcia
991551	Female	Arctic	Pt. Hope- Tigara	AMNH	Garcia
991569	Female	Arctic	Pt. Hope- Tigara	AMNH	Garcia
991644	Male	Arctic	Pt. Hope- Tigara	AMNH	Garcia
991667	Female	Arctic	Pt. Hope- Tigara	AMNH	Garcia
991671	Female	Arctic	Pt. Hope- Tigara	AMNH	Garcia
991672	Female	Arctic	Pt. Hope- Tigara	AMNH	Garcia
991675	Female	Arctic	Pt. Hope- Tigara	AMNH	Garcia
P381094	Male	Arctic	Barrow- Kugusugaruk	NMNH	Hunt
P381097	Unknown	Arctic	Barrow - Kugusugaruk	NMNH	Hunt
P381098	Male	Arctic	Barrow - Kugusugaruk	NMNH	Hunt
P381101	Male	Arctic	Barrow - Kugusugaruk	NMNH	Hunt
P381102	Male	Arctic	Barrow - Kugusugaruk	NMNH	Hunt
P381103	Unknown	Arctic	Barrow - Kugusugaruk	NMNH	Hunt
P381106	Male	Arctic	Barrow - Kugusugaruk	NMNH	Hunt
P381107	Unknown	Arctic	Barrow - Kugusugaruk	NMNH	Hunt
P381111	Unknown	Arctic	Barrow - Nunavak	NMNH	Hunt
P381112	Male	Arctic	Barrow - Kugusugaruk	NMNH	Hunt
P381117	Male	Arctic	Barrow - Kugusugaruk	NMNH	Hunt
P381125	Male	Arctic	Barrow - Kugusugaruk	NMNH	Hunt
P381129	Male	Arctic	Barrow - Kugusugaruk	NMNH	Hunt
P381130	Male	Arctic	Barrow - Kugusugaruk	NMNH	Hunt

East Asian Ancestry Specimens

Buriat and Urga skulls were scanned by Drs. Lauren Butaric and Bruno Frohlich and stored in the National Museum of Natural History (Washington, D.C.).

Table 10. The East Asian Collection, Credited Sources, and Archivists

ID	SEX	REGION	POPULATION	MUSEUM	SCANNER
P278701	Female	Asia	Buriat- Troiskosavsk	NMNH	Butaric
P278702	Female	Asia	Buriat - Troiskosavsk	NMNH	Butaric
P278703	Female	Asia	Buriat - Troiskosavsk	NMNH	Butaric
P278704	Female	Asia	Buriat - Troiskosavsk	NMNH	Butaric
P278705	Male	Asia	Buriat - Troiskosavsk	NMNH	Butaric
P278707	Female	Asia	Buriat - Troiskosavsk	NMNH	Butaric
P278708	Male	Asia	Buriat - Troiskosavsk	NMNH	Butaric
P278709	Female	Asia	Buriat - Troiskosavsk	NMNH	Butaric
P278710	Male	Asia	Buriat - Troiskosavsk	NMNH	Butaric
P278711	Male	Asia	Buriat - Troiskosavsk	NMNH	Butaric
P278712	Female	Asia	Buriat - Troiskosavsk	NMNH	Butaric
P278713	Female	Asia	Buriat - Troiskosavsk	NMNH	Butaric
P278716	Male	Asia	Buriat - Troiskosavsk	NMNH	Butaric
P283601	Female	Asia	Buriat- Kyatchta	NMNH	Butaric
P283603	Female	Asia	Buriat - Kyatchta	NMNH	Butaric
P283604	Male	Asia	Buriat - Kyatchta	NMNH	Butaric
P283606	Male	Asia	Buriat - Kyatchta	NMNH	Butaric
P283607	Male	Asia	Buriat - Kyatchta	NMNH	Butaric
P283610	Female	Asia	Buriat - Kyatchta	NMNH	Butaric
P283614	Male	Asia	Buriat - Kyatchta	NMNH	Butaric
P283615	Male	Asia	Buriat - Kyatchta	NMNH	Butaric
P283617	Male	Asia	Buriat - Kyatchta	NMNH	Butaric
P283623	Female	Asia	Buriat - Kyatchta	NMNH	Butaric
P278720	Female	Asia	Mongolian-Urga	NMNH	Frohlich
P278724	Male	Asia	Mongolian- Urga	NMNH	Frohlich
P278733	Female	Asia	Mongolian- Urga	NMNH	Frohlich
P278738	Female	Asia	Mongolian- Urga	NMNH	Frohlich
P278739	Female	Asia	Mongolian- Urga	NMNH	Frohlich
P278740	Male	Asia	Mongolian- Urga	NMNH	Frohlich
P278744	Male	Asia	Mongolian- Urga	NMNH	Frohlich
P278745	Male	Asia	Mongolian- Urga	NMNH	Frohlich
P278746	Female	Asia	Mongolian- Urga	NMNH	Frohlich
P278747	Male	Asia	Mongolian- Urga	NMNH	Frohlich
P278749	Female	Asia	Mongolian- Urga	NMNH	Frohlich

P278750	Female	Asia	Mongolian- Urga	NMNH	Frohlich
P278753	Female	Asia	Mongolian- Urga	NMNH	Frohlich
P278757	Male	Asia	Mongolian- Urga	NMNH	Frohlich
P278900	Male	Asia	Mongolian- Urga	NMNH	Frohlich
P278901	Male	Asia	Mongolian- Urga	NMNH	Frohlich
P278903	Female	Asia	Mongolian- Urga	NMNH	Frohlich
P278905	Female	Asia	Mongolian- Urga	NMNH	Frohlich
P278907	Male	Asia	Mongolian- Urga	NMNH	Frohlich

European Ancestry Specimens:

Dalmatian and Bosnian skulls scanned by Dr. Lauren Butaric and stored in American Museum of Natural History (New York City, N.Y.). German and Scandinavian skulls were either scanned by Drs. Janet Monge and Tom Schoenemann of the Open Resource Scan Archive at University of Pennsylvania (Philadelphia, P.A.) or scanned by NESPOS and stored in Leizpeg Museum. The North American skulls were scanned by Dr. Butaric and stored in the National Museum of Natural History (Washington, D.C.).

Table 11. European Collection, Credited Sources, and Archivists

ID	SEX	REGION	POPULATION	MUSEUM	SCANNED BY
VL0289	Female	Europe	Dalmatia	AMNH	Butaric
VL0293	Male	Europe	Dalmatia	AMNH	Butaric
VL0295	Male	Europe	Dalmatia	AMNH	Butaric
VL0296	Female	Europe	Dalmatia	AMNH	Butaric
VL0297	Male	Europe u	Dalmatia European	AMNH	Butaric
VL0300	Female	Europe u	Dalmatia European	AMNH	Butaric
VL0306	Male	Europe	Dalmatia	AMNH	Butaric
VL0309	Male	Europe	Dalmatia	AMNH	Butaric
VL0310	Unknown	Europe	Dalmatia	AMNH	Butaric
VL0313	Male	Europe	Dalmatia	AMNH	Butaric
VL0318	Unknown	Europe	Dalmatia	AMNH	Butaric
VL0319	Female	Europe	Dalmatia	AMNH	Butaric
VL0330	Male	Europe	Dalmatia	AMNH	Butaric
VL0331	Male	Europe	Dalmatia	AMNH	Butaric
VL0332	Male	Europe	Dalmatia	AMNH	Butaric
VL0333	Male	Europe	Dalmatia	AMNH	Butaric
VL3292	Male	Europe	Bosnia	AMNH	Butaric

MOR0037	Female	Europe	Germany	Penn	ORSA
MOR0706	Male	Europe	Germany	Penn	ORSA
MOR1063	Male	Europe	Germany	Penn	ORSA
MOR1252	Female	Europe	Finland	Penn	ORSA
MOR1487	Female	Europe	Sweden	Penn	ORSA
MOR1534	Male	Europe	Finland	Penn	ORSA
MOR1540	Male	Europe	Finland	Penn	ORSA
ULAC013	Female	Europe	Germany	Leizpeig	NESPOS
ULAC016	Male	Europe	Germany	Leizpeig	NESPOS
ULAC019	Male	Europe	Germany	Leizpeig	NESPOS
ULAC033	Male	Europe	Netherlands	Leizpeig	NESPOS
ULAC039	Female	Europe	Netherlands	Leizpeig	NESPOS
ULAC057	Male	Europe	Norway/Sweden	Leizpeig	NESPOS
ULAC058	Male	Europe	Norway/Sweden	Leizpeig	NESPOS
ULAC060	Male	Europe	Norway/Sweden	Leizpeig	NESPOS
ULAC066	Female	Europe	Norway/Sweden	Leizpeig	NESPOS
TC651	Male	Europe	North America	NMNH	Butaric
TC713	Male	Europe	North America	NMNH	Butaric
TC813	Male	Europe	North America	NMNH	Butaric
TC814	Male	Europe	North America	NMNH	Butaric
TC843	Male	Europe	North America	NMNH	Butaric
TC853	Male	Europe	North America	NMNH	Butaric
TC867	Male	Europe	North America	NMNH	Butaric
TC868	Male	Europe	North America	NMNH	Butaric
TC879	Male	Europe	North America	NMNH	Butaric
TC880	Female	Europe	North America	NMNH	Butaric
TC904R	Female	Europe	North America	NMNH	Butaric
TC908	Male	Europe	North America	NMNH	Butaric
TC918	Male	Europe	North America	NMNH	Butaric
TC956	Male	Europe	North America	NMNH	Butaric
TC1028	Male	Europe	North America	NMNH	Butaric
TC1089	Male	Europe	North America	NMNH	Butaric
TC1120	Female	Europe	North America	NMNH	Butaric

APPENDIX B: SKULL MEASUREMENTS

Table 12. Collected Measurements for Specimens in Study. SEB: Total (Tot), left (L), right (R), average of left and right sides (Avg). FEB: left and right ethmoidal air cells (EAC), superior (SM) and superior common (CM) meatuses, and totals; average of left and right sides. Nasal Breadth (NB). Nasal Height(NH): average, left, and right.

The Arctic Circle															
	SEB				*FEB*	*L FEB*				*R FEB*				*FEB*	*NB*
	Tot	*L*	*R*	*Avg*	*Tot*	*EAC*	*SM*	*CM*	*Tot*	*CM*	*SM*	*EAC*	*Tot*	*Avg*	
99187	23.4	12.0	11.4	11.7	23.0	5.9	3.7	2.4	12.0	2.9	2.4	5.8	11.1	11.5	30.2
991102	24.8	11.7	13.2	12.4	26.2	6.3	2.8	3.7	12.8	3.6	2.8	6.9	13.4	13.1	30.9
991103	22.0	11.1	11.0	11.0	21.8	4.6	3.1	3.1	10.8	2.9	2.8	5.3	11.0	10.9	30.6
991166	23.3	11.4	12.0	11.7	24.3	6.2	2.5	2.9	11.6	2.6	3.2	6.9	12.7	12.1	29.4
991168	22.0	10.8	11.2	11.0	21.8	5.9	3.3	2.2	11.3	2.0	4.4	4.0	10.5	10.9	30.3
991181	23.5	11.5	12.0	11.8	23.9	4.4	2.7	4.4	11.4	4.8	2.8	5.0	12.6	12.0	33.9
991194	23.8	11.8	12.0	11.9	26.1	7.1	2.4	3.2	12.8	5.1	4.0	4.2	13.3	13.1	34.4
991197	22.7	11.4	11.6	11.5	22.7	4.8	2.7	3.9	11.5	4.0	3.0	4.5	11.5	11.5	31.9
991199	22.6	10.6	12.0	11.3	24.8	2.4	3.4	6.4	12.2	4.5	3.7	4.5	12.6	12.4	29.6
991224	22.2	10.3	11.9	11.1	21.7	4.0	2.6	3.7	10.2	3.2	3.5	4.8	11.5	10.9	31.0
991234	20.7	10.2	10.6	10.4	22.4	6.6	2.8	2.3	11.6	3.2	3.3	4.3	10.8	11.2	30.7
991235	25.7	13.0	12.7	12.9	26.1	5.5	3.4	5.3	14.2	3.4	3.9	4.6	11.9	13.1	33.7
991237	26.1	13.4	12.8	13.1	26.4	6.2	2.6	3.8	12.5	3.2	4.3	6.5	14.0	13.3	29.2
991240	22.5	11.4	11.1	11.3	29.4	7.5	4.1	3.0	14.7	6.7	4.0	4.1	14.8	14.7	33.2
991248	19.8	9.6	10.3	9.9	21.8	5.6	2.7	2.5	10.8	2.7	2.1	6.2	11.0	10.9	29.8
991250	22.8	11.1	11.7	11.4	23.7	4.4	4.0	3.5	11.8	3.3	4.7	4.0	12.0	11.9	30.6
991252	23.2	12.0	11.2	11.6	24.0	5.6	3.4	4.0	13.1	3.4	2.0	5.7	11.0	12.0	32.2
991257	18.2	9.7	8.5	9.1	21.4	5.4	2.7	2.7	10.8	2.0	2.1	6.5	10.6	10.7	29.8
991260	20.6	9.8	10.8	10.3	20.4	3.3	3.6	2.1	9.0	3.9	4.9	2.6	11.4	10.2	35.8
991262	22.8	11.1	11.8	11.5	22.9	4.8	4.4	2.7	12.0	1.8	3.7	5.4	10.9	11.4	32.8
991268	23.7	11.4	12.2	11.8	26.9	7.1	3.3	2.9	13.4	1.8	2.1	9.9	13.8	13.6	32.5
991276	20.8	10.0	10.9	10.4	21.1	4.0	3.2	3.7	10.9	2.3	2.9	5.0	10.2	10.6	26.9
991277	25.1	12.1	13.0	12.5	29.1	9.9	2.6	2.4	15.0	1.7	2.2	10.2	14.1	14.6	31.3
991278	22.6	10.5	12.1	11.3	21.2	4.9	3.1	2.6	10.6	3.0	2.3	5.2	10.6	10.6	25.3
991282	20.8	10.1	10.8	10.4	24.6	5.8	2.6	3.0	11.4	2.4	2.6	8.3	13.2	12.3	34.0
991296	19.1	9.2	9.9	9.6	23.9	3.5	3.3	3.1	9.9	3.6	3.3	7.2	14.0	12.0	27.4
991324	24.2	12.3	11.9	12.1	25.7	6.4	3.3	4.3	14.0	2.1	4.1	5.5	11.7	12.9	31.2
991330	23.7	12.5	11.2	11.9	28.5	8.1	3.7	2.5	14.3	3.2	3.3	7.6	14.2	14.3	31.8
991332	22.2	10.9	11.4	11.1	22.4	4.9	3.7	3.3	11.9	2.2	2.3	6.1	10.6	11.2	30.4
991334	22.0	11.8	10.2	11.0	22.1	5.0	3.5	3.7	12.2	3.0	2.7	4.2	9.9	11.0	37.3
991335	21.9	11.0	11.1	11.0	26.2	8.5	2.1	2.3	13.0	2.8	2.1	8.3	13.2	13.1	32.2
991336	25.1	12.5	12.6	12.5	22.4	5.5	2.4	3.2	11.0	3.5	2.2	5.6	11.4	11.2	30.6
991339	24.1	11.3	12.9	12.1	29.1	9.2	3.1	2.6	14.9	2.8	2.4	9.1	14.3	14.6	30.0
991340	26.9	14.0	12.9	13.5	28.0	7.1	4.2	3.7	15.0	4.2	3.1	5.6	13.0	14.0	28.8
991345	25.2	12.5	12.7	12.6	28.1	6.2	3.6	4.7	14.5	4.9	3.5	5.3	13.7	14.1	24.5
991346	24.8	11.8	13.2	12.5	27.5	7.5	3.7	3.9	15.1	4.1	3.7	4.6	12.4	13.8	30.6

	SEB				FEB	L FEB				R FEB				FEB	NB
	Tot	*L*	*R*	*Avg*	*Tot*	*EAC*	*SM*	*CM*	*Tot*	*CM*	*SM*	*EAC*	*Tot*	*Avg*	
991355	22.9	11.8	11.0	11.4	23.3	5.5	2.7	3.7	11.8	3.5	3.3	4.7	11.5	11.7	27.5
991357	24.8	11.4	13.4	12.4	28.9	8.2	2.4	3.7	14.4	2.6	2.5	9.4	14.6	14.5	32.3
991362	23.2	11.9	11.3	11.6	26.4	7.2	3.3	3.9	14.5	2.8	2.8	6.4	12.0	13.2	29.6
991364	24.8	12.6	12.2	12.4	23.5	6.1	2.9	3.1	12.1	2.9	2.3	6.2	11.4	11.8	32.6
991373	28.7	13.0	15.8	14.4	25.6	6.5	2.5	2.9	11.8	3.6	2.6	7.6	13.8	12.8	32.6
991459	23.8	11.1	12.7	11.9	24.7	4.8	1.9	5.4	12.0	3.3	2.7	6.6	12.7	12.3	30.4
991510	25.8	13.0	12.9	12.9	28.5	7.1	2.3	4.7	14.1	4.8	3.0	6.6	14.4	14.3	29.0
991511	23.3	11.1	12.2	11.6	22.7	4.4	3.0	2.3	9.8	3.8	2.6	6.5	12.9	11.3	26.9
991513	21.2	10.6	10.6	10.6	22.6	6.1	2.2	3.3	11.6	3.1	1.7	6.2	11.1	11.3	27.5
991515	22.3	11.8	10.6	11.2	23.6	6.1	2.3	3.1	11.6	2.9	2.3	6.8	12.0	11.8	36.6
991519	23.9	11.9	12.0	12.0	25.8	6.4	3.3	3.6	13.3	3.0	3.2	6.3	12.5	12.9	33.2
991520	20.2	9.4	10.8	10.1	24.8	7.5	2.6	2.0	12.1	2.5	2.7	7.5	12.6	12.4	31.3
991524	21.2	10.2	10.9	10.6	22.9	6.1	2.6	2.5	11.2	2.1	2.9	6.8	11.7	11.5	30.9
991525	22.4	10.7	11.7	11.2	26.3	6.2	1.8	3.9	11.9	5.1	2.5	6.7	14.4	13.1	30.3
991526	24.5	11.7	12.8	12.3	28.3	9.8	1.5	3.7	15.0	3.2	2.5	7.6	13.3	14.2	30.4
991542	24.3	12.2	12.1	12.2	27.4	8.3	1.8	3.3	13.4	3.1	2.5	8.4	14.0	13.7	30.4
991546	19.9	9.6	10.2	9.9	20.5	5.5	2.2	2.4	10.1	3.2	2.7	4.6	10.4	10.2	28.2
991549	25.9	12.3	13.6	12.9	24.8	6.1	2.0	3.0	11.1	4.0	1.7	8.0	13.7	12.4	26.2
991551	21.6	10.7	11.0	10.8	21.5	5.8	2.1	2.4	10.3	2.8	2.4	5.9	11.1	10.7	33.1
991569	21.6	10.2	11.5	10.8	25.0	3.3	3.3	5.2	11.8	4.8	4.0	4.4	13.2	12.5	34.0
991644	22.9	11.0	11.9	11.5	22.3	6.9	2.6	2.2	11.7	2.9	2.9	4.7	10.6	11.1	28.9
991667	24.6	12.3	12.3	12.3	30.8	9.2	2.2	3.0	14.4	3.0	2.4	11.0	16.4	15.4	31.6
991671	23.7	10.7	13.0	11.9	25.0	4.3	3.6	5.0	12.8	4.5	3.1	4.6	12.2	12.5	31.4
991672	21.8	11.0	10.8	10.9	26.9	7.8	2.6	1.8	12.2	2.7	3.5	8.6	14.7	13.5	35.2
991675	22.9	12.2	10.7	11.5	23.3	8.3	2.5	1.8	12.7	2.4	1.6	6.7	10.7	11.7	31.9
P381094	20.6	8.7	11.9	10.3	24.6	7.9	2.1	1.5	11.6	2.7	2.1	8.2	13.0	12.3	35.3
P381097	25.8	12.8	13.3	13.0	32.2	9.9	3.9	3.4	17.2	2.3	3.2	9.5	15.0	16.1	31.8
P381098	24.4	11.6	13.0	12.3	25.1	6.9	1.8	3.6	12.4	3.2	2.7	6.9	12.7	12.6	33.0
P381101	26.0	12.6	13.4	13.0	29.3	9.8	3.1	2.2	15.1	2.2	2.7	9.3	14.2	14.7	34.2
P381102	24.8	11.7	13.2	12.4	26.2	6.3	2.8	3.7	12.8	3.6	2.8	6.9	13.4	13.1	30.9
P381103	19.4	9.1	10.3	9.7	21.4	4.6	2.6	2.7	9.9	4.6	3.3	3.7	11.6	10.7	33.1
P381106	23.0	11.2	11.7	11.5	26.6	9.5	1.6	1.7	12.8	2.6	1.6	9.5	13.8	13.3	26.5
P381107	19.1	8.4	10.7	9.5	20.6	4.8	2.1	2.6	9.5	3.0	1.9	6.1	11.1	10.3	30.5
P381111	24.9	11.8	13.2	12.5	25.6	8.4	2.1	2.7	13.2	3.0	3.5	5.9	12.4	12.8	30.7
P381112	22.9	11.2	11.7	11.5	25.9	7.3	1.8	3.8	12.9	3.7	3.7	5.5	12.9	12.9	31.4
P381117	23.7	11.6	12.1	11.9	26.6	9.2	1.9	2.7	13.8	2.9	1.5	8.4	12.8	13.3	30.4
P381125	27.6	14.0	13.6	13.8	26.0	7.6	2.6	2.6	12.8	3.7	2.5	6.9	13.2	13.0	32.0
P381129	21.7	11.5	10.2	10.8	21.2	5.4	2.7	3.5	11.6	2.6	2.7	4.3	9.6	10.6	30.1
P381130	22.6	11.5	11.2	11.3	24.9	7.4	3.1	3.5	14.0	2.6	2.8	5.5	10.9	12.5	33.2

Europe																
	SEB				*FEB*	*L FEB*				*R FEB*				*FEB*	*NB*
	Tot	*L*	*R*	*Avg*	*Tot*	*EAC*	*SM*	*CM*	*Tot*	*CM*	*SM*	*EAC*	*Tot*	*Avg*	
VL0289	29.1	11.6	11.3	11.5	28.9	10.0	2.3	2.3	14.6	2.5	2.0	9.9	14.4	14.5	35.6
VL0293	27.0	13.7	13.2	13.5	25.9	6.2	3.4	3.8	13.4	4.0	2.9	6.0	12.9	13.1	34.4
VL0295	23.8	10.7	13.0	11.9	22.3	3.4	3.8	3.6	10.9	2.8	4.9	3.8	11.4	11.2	30.4
VL0296	24.6	11.9	12.8	12.3	24.9	4.1	3.3	5.3	12.7	4.6	4.0	3.7	12.2	12.4	31.2
VL0297	26.8	13.5	13.4	13.4	27.3	6.3	3.5	3.4	13.2	4.1	4.3	5.8	14.2	13.7	30.8
VL0306	30.0	16.3	13.8	15.0	29.5	9.8	2.8	3.8	16.4	3.0	2.4	7.7	13.1	14.7	36.6
VL0309	23.0	10.9	12.1	11.5	21.9	5.6	1.8	4.1	11.4	3.2	2.3	5.0	10.5	11.0	30.0
VL0310	27.6	13.5	14.1	13.8	26.9	5.7	4.0	3.0	12.7	4.1	3.2	6.8	14.2	13.5	30.1
VL0313	26.7	12.9	13.8	13.4	26.7	7.1	2.6	4.0	13.7	2.8	2.3	8.0	13.1	13.4	32.7
VL0318	28.0	13.3	14.7	14.0	28.8	5.7	3.5	4.4	13.6	3.5	4.1	7.6	15.1	14.4	36.8
VL0319	27.0	12.1	15.0	13.6	27.3	7.1	2.2	2.0	11.4	2.2	2.1	11.6	15.9	13.6	35.2
VL0330	22.7	11.6	11.2	11.4	23.6	5.8	3.3	3.6	12.7	3.5	3.0	4.4	10.9	11.8	34.9
VL0331	26.4	12.3	14.3	13.3	26.6	6.5	2.2	3.7	12.4	4.1	2.7	7.4	14.3	13.3	36.7
Vl0332	26.2	13.3	12.9	13.1	26.8	10.3	1.8	2.5	14.6	3.0	2.2	6.9	12.1	13.4	34.1
VL0333	23.6	12.1	11.5	11.8	22.9	5.3	2.9	3.7	11.9	3.2	2.8	5.1	11.1	11.5	33.8
VL3292	26.2	14.1	12.2	13.1	25.3	6.6	3.0	3.8	13.4	4.0	2.6	5.5	12.0	12.7	33.7
Mor0037	27.2	11.9	15.4	13.6	23.4	6.1	2.7	2.3	11.1	3.1	1.7	7.5	12.3	11.7	35.9
Mor0706	25.0	12.1	13.0	12.5	25.5	5.7	3.2	3.4	12.3	3.5	2.8	6.8	13.2	12.8	31.1
Mor1063	26.5	13.2	13.3	13.2	26.4	6.1	2.7	4.7	13.6	4.6	4.0	4.4	12.9	13.2	32.3
Mor1252	21.0	10.4	10.6	10.5	21.1	4.7	2.3	3.0	10.0	3.2	2.9	5.0	11.1	10.6	34.3
Mor1487	25.5	11.8	13.6	12.7	23.6	5.3	2.8	3.1	11.2	2.7	3.4	6.3	12.4	11.8	29.3
Mor1534	23.8	12.0	11.8	11.9	21.5	7.1	1.5	2.7	11.4	2.4	2.2	5.5	10.1	10.7	29.9
Mor1540	23.7	11.6	12.0	11.8	23.3	6.7	2.2	2.5	11.3	3.4	3.2	5.5	12.0	11.6	32.4
ULAC013	23.7	10.8	13.0	11.9	29.0	7.0	3.3	3.2	13.4	3.2	4.5	7.9	15.6	14.5	27.2
ULAC016	25.2	13.9	11.4	12.6	24.2	6.5	3.0	3.7	13.2	3.1	4.5	3.5	11.2	12.2	30.1
ULAC019	24.8	12.2	12.6	12.4	26.1	5.4	3.9	3.1	12.4	3.4	3.1	7.2	13.7	13.0	34.1
ULAC033	23.3	12.4	11.3	11.9	24.6	6.6	2.8	3.8	13.2	3.4	3.1	5.0	11.5	12.3	35.2
ULAC039	25.2	13.2	12.0	12.6	26.1	5.9	3.6	3.9	13.4	4.0	3.2	5.5	12.7	13.1	35.4
ULAC057	29.7	15.1	14.6	14.8	26.6	6.7	3.5	4.7	14.8	4.6	2.9	4.3	11.8	13.3	40.4
ULAC058	22.3	11.0	11.4	11.2	25.0	5.8	3.1	4.5	13.4	4.2	4.8	2.5	11.6	12.5	31.5
ULAC060	24.2	11.5	12.7	12.1	25.7	6.6	3.3	2.7	12.6	2.6	3.4	7.0	13.0	12.8	37.4
ULAC066	25.1	11.9	13.2	12.6	25.9	7.0	2.2	3.4	12.7	2.4	2.2	8.7	13.4	13.0	31.9
TC651	27.5	13.1	14.4	13.7	26.3	5.9	4.1	3.1	13.0	3.4	3.3	6.6	13.3	13.2	36.3
TC713	26.9	12.9	14.0	13.5	30.1	8.6	3.4	4.4	16.4	3.6	4.2	5.9	13.8	15.1	35.8
TC813	27.2	13.4	13.8	13.6	26.4	6.1	3.8	3.9	13.8	2.2	2.2	8.2	12.6	13.2	37.1
TC814	25.5	13.1	12.4	12.7	25.1	5.8	3.7	3.6	13.1	3.3	4.6	4.1	12.1	12.6	27.7
TC843	25.9	11.9	14.0	13.0	24.4	5.6	2.9	3.5	12.1	3.6	2.5	6.2	12.3	12.2	29.2
TC853	22.3	10.8	11.5	11.2	24.4	5.7	2.8	4.0	12.6	3.4	2.1	6.3	11.9	12.2	30.3
TC867	27.1	13.0	14.2	13.6	27.8	7.1	3.2	2.7	13.0	4.6	2.7	7.5	14.8	13.9	32.6
TC868	26.9	12.9	14.0	13.5	30.1	8.6	3.4	4.4	16.4	3.6	4.2	5.9	13.8	15.1	35.8
TC879	23.5	11.5	12.0	11.8	23.9	6.9	2.5	2.5	11.9	2.5	2.1	7.4	12.1	12.0	29.7
TC880	22.3	10.9	11.4	11.1	24.3	6.1	2.9	2.2	11.1	3.7	3.7	5.9	13.3	12.2	28.0
TC904R	26.6	11.1	15.9	13.5	25.9	6.9	2.9	3.3	13.0	3.5	3.1	6.3	12.9	13.0	29.3

TC908	21.5	10.9	10.5	10.7	21.5	5.0	2.4	3.1	10.5	3.6	3.1	4.3	11.0	10.8	38.7
TC918	31.1	15.7	15.4	15.6	30.2	6.8	2.4	4.8	14.0	3.7	2.8	9.8	16.3	15.1	35.7
TC956	24.8	11.0	13.8	12.4	22.1	4.7	2.4	3.7	10.8	3.2	2.7	5.4	11.4	11.1	34.5
TC1028	26.4	11.9	14.5	13.2	26.9	4.1	3.1	5.0	12.2	4.5	3.0	7.3	14.8	13.5	34.0
TC1089	23.4	11.4	12.0	11.7	22.1	4.4	3.1	3.5	11.0	3.2	3.5	4.5	11.2	11.1	28.9

Equatorial Africa															
	SEB				*FEB*	*L FEB*				*R FEB*				*FEB*	*NB*
	Tot	*L*	*R*	*Avg*	*Tot*	*EAC*	*SM*	*CM*	*Tot*	*CM*	*SM*	*EAC*	*Tot*	*Avg*	
MOR0645	31.2	15.0	16.3	15.6	32.9	10.3	2.5	3.5	16.2	2.8	4.0	9.8	16.6	16.4	32.0
MOR0646	28.4	13.1	15.4	14.2	29.5	6.8	4.0	3.3	14.0	4.1	5.4	6.0	15.4	14.7	38.3
MOR0647	32.2	15.4	16.9	16.1	35.4	11.0	3.0	3.6	17.6	4.0	2.5	11.3	17.8	17.7	38.5
MOR0914	27.7	13.8	13.9	13.9	30.4	9.1	2.5	3.7	15.3	4.2	2.2	8.8	15.2	15.2	32.4
MOR0915	29.2	14.2	15.0	14.6	31.2	8.3	2.8	4.1	15.2	3.7	3.0	9.4	16.1	15.6	32.2
MOR0917	31.6	15.6	16.1	15.9	35.8	10.0	3.6	3.8	17.5	4.2	2.9	11.2	18.3	17.9	29.0
MOR0920	30.7	16.0	14.7	15.4	30.8	9.8	2.9	3.0	15.7	2.6	3.1	9.4	15.1	15.4	33.0
MOR0923	25.4	12.0	13.5	12.7	24.8	6.9	2.6	3.1	12.5	3.1	3.4	5.7	12.3	12.4	29.7
MOR0924	25.2	12.7	12.7	12.7	26.3	9.4	2.5	1.9	13.8	2.5	2.4	7.5	12.5	13.1	32.4
MOR0925	31.1	15.4	15.7	15.5	31.8	8.7	3.3	4.5	16.5	3.8	3.3	8.2	15.4	15.9	40.0
MOR0927	23.8	11.6	12.2	11.9	25.9	7.1	4.0	2.6	13.7	2.7	4.3	5.3	12.2	13.0	38.5
MOR0963	23.5	12.1	11.5	11.8	26.8	7.8	3.8	1.7	13.3	3.0	3.2	7.3	13.5	13.4	33.0
MOR0964	31.8	17.3	14.5	15.9	33.3	11.6	4.0	2.7	18.4	3.3	3.2	8.5	15.0	16.7	42.7
MOR0968	28.3	14.5	13.8	14.2	31.7	10.1	3.5	2.5	16.0	2.9	3.5	9.3	15.7	15.9	35.5
MOR0971	29.1	14.1	15.1	14.6	27.9	7.4	2.8	3.6	13.8	3.3	3.7	7.1	14.1	14.0	27.1
Mor0974	29.0	14.1	14.9	14.5	30.4	9.5	2.4	2.5	14.4	3.4	1.9	10.7	16.0	15.2	33.1
Mor0975	22.4	10.6	11.7	11.2	22.8	3.2	3.2	3.5	9.9	4.0	3.8	5.1	12.9	11.4	22.9
Mor0976	25.1	12.1	13.1	12.6	25.6	4.4	2.7	5.2	12.2	4.9	2.4	6.2	13.5	12.9	34.2
Mor0978	28.8	14.1	14.8	14.4	30.2	7.7	2.2	3.5	13.4	3.5	3.9	9.3	16.7	15.1	32.9
MOR0993	30.0	14.4	15.8	15.1	32.4	9.4	3.5	3.4	16.4	3.2	3.8	9.1	16.0	16.2	36.1
Mor0994	28.1	14.4	13.7	14.1	28.4	7.8	2.8	4.3	14.9	3.9	2.8	6.7	13.5	14.2	31.8
MOR1100	26.8	13.6	13.3	13.4	28.4	6.3	3.0	3.9	13.2	4.1	3.7	7.3	15.1	14.2	36.9
MOR1102	29.7	15.0	14.7	14.8	32.2	12.1	1.8	2.7	16.6	2.4	2.2	11.0	15.6	16.1	25.5
P049446	26.6	14.0	12.6	13.3	27.3	9.1	1.7	3.8	14.6	4.0	2.7	6.1	12.8	13.7	37.0
P244050	26.1	13.3	12.8	13.1	29.8	9.8	2.8	3.6	16.2	3.1	2.7	7.7	13.6	14.9	33.4
P244052	29.8	14.8	14.9	14.9	29.0	7.2	3.5	3.9	14.6	5.2	3.0	6.2	14.4	14.5	25.5
P244055	29.4	14.3	15.1	14.7	28.4	7.9	2.7	3.6	14.1	4.3	2.9	7.0	14.2	14.2	35.7
P244057	25.4	12.8	12.7	12.7	27.7	7.3	2.2	3.9	13.5	3.3	2.7	8.2	14.2	13.8	37.8
P276088	27.0	13.1	13.9	13.5	27.5	7.8	4.1	2.4	14.2	3.5	4.6	5.2	13.3	13.8	34.8
P276090	26.6	13.0	13.6	13.3	25.0	6.7	2.1	2.9	11.7	3.8	2.3	7.2	13.3	12.5	29.0
P276092	26.3	12.6	13.7	13.2	24.5	4.7	3.7	2.9	11.3	3.5	5.2	4.6	13.2	12.2	26.7
P276093	20.2	9.3	10.9	10.1	21.9	4.7	2.7	1.9	9.3	3.5	3.8	5.4	12.7	11.0	34.6
P276348	26.4	12.2	14.2	13.2	29.8	7.6	3.0	3.6	14.2	2.5	4.2	8.9	15.6	14.9	31.6
P302767	30.1	15.3	14.8	15.0	29.2	9.3	2.2	3.1	14.6	2.9	3.0	8.7	14.6	14.6	28.3
P323695	30.1	15.4	14.7	15.1	31.8	7.2	3.9	4.4	15.6	4.2	4.2	7.9	16.2	15.9	36.9
P381071	23.4	13.2	10.2	11.7	30.2	9.4	3.0	2.0	14.4	4.2	3.0	8.5	15.7	15.1	28.4

	SEB				*FEB*	*L FEB*				*R FEB*				*FEB*	*NB*
	Tot	*L*	*R*	*Avg*	*Tot*	*EAC*	*SM*	*CM*	*Tot*	*CM*	*SM*	*EAC*	*Tot*	*Avg*	
P381074	29.8	14.3	15.6	14.9	30.7	4.5	5.6	5.0	15.1	4.3	5.2	6.1	15.6	15.4	36.7
P381076	26.2	12.0	14.1	13.1	26.2	5.3	3.4	2.6	11.4	5.2	2.6	7.0	14.8	13.1	29.5
P257540	28.6	14.9	13.7	14.3	30.7	12.3	1.7	3.0	17.0	2.1	3.0	8.5	13.6	15.3	40.2
P257548	24.8	11.7	13.2	12.4	26.2	6.3	2.8	3.7	12.8	3.6	2.8	6.9	13.4	13.1	30.9
P257549	24.9	12.4	12.4	12.4	25.6	4.7	3.2	3.7	11.7	4.9	3.5	5.6	13.9	12.8	31.2
P257584	32.5	16.4	16.2	16.3	35.6	13.9	1.6	2.8	18.2	2.3	2.9	12.3	17.5	17.8	39.9
P257587	27.9	13.6	14.3	14.0	28.8	7.7	2.9	3.4	14.0	5.1	3.1	6.6	14.8	14.4	37.4
P257588	30.3	15.8	14.6	15.2	32.2	11.4	3.6	3.2	18.2	3.1	3.7	7.2	14.0	16.1	39.8
P257591	31.1	15.8	15.3	15.6	30.3	7.0	3.5	3.7	14.2	5.2	3.4	7.4	16.1	15.2	37.2
P257594	28.4	14.6	13.8	14.2	29.3	8.9	2.7	3.6	15.1	3.5	2.6	8.1	14.1	14.6	30.4
P257599	27.5	13.0	14.5	13.8	27.5	7.4	3.1	3.7	14.2	3.5	4.3	5.5	13.3	13.8	32.9
P273199	26.1	12.2	13.9	13.1	25.2	6.3	2.9	3.0	12.2	3.5	3.6	5.8	12.9	12.6	30.2
P273205	29.4	15.1	14.3	14.7	29.8	7.9	3.6	3.6	15.1	4.3	3.2	7.2	14.7	14.9	34.7
P273207	32.9	16.1	16.9	16.5	32.4	9.0	3.4	3.5	15.8	4.0	3.5	9.1	16.6	16.2	36.7

East Asia															
	SEB				*FEB*	*L FEB*				*R FEB*				*FEB*	*NB*
	Tot	*L*	*R*	*Avg*	*Tot*	*EAC*	*SM*	*CM*	*Tot*	*CM*	*SM*	*EAC*	*Tot*	*Avg*	
P278701	26.5	13.6	13.7	13.7	28.7	6.9	2.1	3.1	12.1	4.3	3.4	8.9	16.6	14.4	29.7
P278702	26.7	12.2	14.4	13.3	28.9	8.3	3.2	2.9	14.4	2.9	3.3	8.4	14.6	14.5	32.8
P278703	26.9	13.8	13.0	13.4	25.8	6.4	3.7	3.5	13.6	3.9	2.9	5.5	12.2	12.9	32.1
P278704	25.1	12.4	12.7	12.6	25.9	6.1	2.5	4.2	12.8	4.6	3.8	4.8	13.2	13.0	36.0
P278705	27.5	14.0	13.6	13.8	27.3	6.9	3.5	3.4	13.8	4.5	3.8	5.3	13.6	13.7	31.9
P278707	24.2	12.0	12.3	12.1	26.3	5.1	2.7	5.0	12.8	5.8	2.9	4.8	13.6	13.2	40.8
P278708	23.5	11.6	11.9	11.7	24.2	5.7	2.9	3.7	12.3	4.1	2.8	5.1	12.0	12.1	27.4
P278709	26.8	13.6	13.2	13.4	27.7	4.3	4.1	5.7	14.1	5.3	4.8	3.5	13.7	13.9	28.1
P278710	27.7	14.5	13.2	13.9	29.5	8.6	3.1	4.3	15.9	3.9	3.4	6.5	13.8	14.8	40.9
P278711	27.7	13.9	13.8	13.9	28.6	5.8	3.6	3.6	12.9	5.7	3.4	6.6	15.7	14.3	34.5
P278712	24.4	12.4	12.1	12.2	27.0	7.9	3.1	3.8	14.8	3.1	3.0	6.2	12.3	13.6	37.3
P278713	23.2	11.9	11.3	11.6	22.8	5.6	2.0	4.6	12.2	3.9	2.6	4.1	10.6	11.4	33.4
P278716	27.2	14.4	12.8	13.6	27.1	9.6	2.5	2.5	14.5	2.9	2.8	6.9	12.6	13.6	31.2
P283601	22.7	11.3	11.4	11.3	20.2	4.6	2.8	3.1	10.5	2.9	2.4	4.4	9.7	10.1	37.1
P283603	24.2	12.9	11.3	12.1	23.4	7.7	3.0	2.2	12.9	2.7	1.8	6.1	10.6	11.7	27.8
P283604	29.4	13.9	15.5	14.7	29.3	7.5	3.3	2.4	13.3	3.0	2.6	10.5	16.2	14.7	39.7
P283606	25.5	12.8	12.8	12.8	27.1	7.2	3.2	4.4	14.8	3.4	3.1	5.9	12.4	13.6	35.5
P283607	30.0	14.1	16.0	15.0	28.7	5.6	3.9	4.5	13.9	5.1	3.8	5.9	14.8	14.4	37.7
P283610	21.0	10.2	10.9	10.5	20.7	3.2	3.2	4.0	10.3	4.3	3.5	2.7	10.4	10.4	34.4
P283614	25.5	12.1	13.4	12.8	29.1	7.1	2.9	4.1	14.1	4.1	3.4	7.5	15.0	14.5	35.8
P283615	28.0	13.1	14.9	14.0	27.0	4.6	3.1	5.1	12.9	4.7	4.3	5.2	14.1	13.5	33.1
P283617	24.0	12.9	11.1	12.0	25.9	3.0	4.2	6.2	13.4	4.9	3.7	3.9	12.6	13.0	36.4
P283623	21.2	10.4	10.8	10.6	20.3	4.7	2.9	2.7	10.3	3.7	2.3	4.0	10.0	10.2	32.3
P278720	26.4	12.4	14.2	13.3	28.2	5.7	3.3	4.9	13.9	4.0	3.9	6.4	14.4	14.1	37.4
P278724	24.5	11.2	13.3	12.3	24.0	5.2	2.3	2.7	10.1	3.4	3.0	7.5	13.9	12.0	32.2

	SEB				*FEB*	*L FEB*				*R FEB*				*FEB*	*NB*
	Tot	*L*	*R*	*Avg*	*Tot*	*EAC*	*SM*	*CM*	*Tot*	*CM*	*SM*	*EAC*	*Tot*	*Avg*	
P278733	24.0	11.9	12.2	12.0	26.1	6.3	2.4	3.7	12.4	2.5	4.6	6.5	13.7	13.1	31.5
P278738	26.6	13.2	13.4	13.3	28.7	10.1	2.7	3.3	16.1	2.2	3.2	7.3	12.7	14.4	34.9
P278739	23.8	11.6	12.2	11.9	25.9	5.7	2.7	3.8	12.2	3.9	3.0	6.8	13.7	13.0	33.4
P278740	24.5	12.5	12.0	12.2	26.7	7.0	3.0	3.4	13.4	4.5	2.3	6.6	13.3	13.3	34.3
P278744	31.9	14.8	17.2	16.0	31.7	8.5	2.7	4.2	15.3	3.8	3.0	9.8	16.6	16.0	31.2
P278745	26.1	12.1	14.0	13.0	28.7	5.0	3.0	5.5	13.4	6.1	3.0	6.4	15.5	14.4	36.5
P278746	25.4	10.6	14.9	12.8	26.8	5.9	2.9	4.4	13.2	4.3	3.0	6.3	13.6	13.4	38.9
P278747	26.1	14.0	12.2	13.1	26.5	5.7	3.5	5.1	14.3	4.3	2.5	5.5	12.2	13.3	37.5
P278749	22.9	10.7	12.1	11.4	21.0	4.1	3.8	3.6	11.5	2.7	2.5	4.6	9.7	10.6	24.9
P278750	24.2	11.9	12.3	12.1	26.6	7.1	3.1	4.0	14.3	3.3	2.7	6.3	12.3	13.3	37.3
P278753	24.6	12.5	12.1	12.3	27.5	4.5	5.0	4.7	14.2	4.1	5.2	4.0	13.3	13.7	34.4
P278757	27.2	12.3	14.9	13.6	25.9	6.3	3.4	3.5	13.2	2.8	3.0	7.0	12.7	13.0	35.3
P278900	26.0	13.3	12.7	13.0	28.1	7.0	4.4	3.5	15.0	4.6	4.5	4.0	13.2	14.1	32.8
P278901	27.8	13.5	14.3	13.9	29.2	8.9	2.4	2.5	13.8	3.6	2.4	9.4	15.5	14.6	36.3
P278903	26.4	12.2	14.1	13.2	28.7	7.5	2.7	3.7	13.8	3.8	4.0	7.1	14.9	14.4	31.8
P278905	22.6	11.4	11.2	11.3	23.7	7.2	2.7	2.3	12.3	2.2	2.2	7.0	11.5	11.9	28.4
P278907	29.2	13.7	15.5	14.6	32.3	9.7	2.5	2.9	15.1	3.1	2.5	11.6	17.2	16.2	35.5

REFERENCES

Ackermann, R., Athreya, S., Bolnick, D., Fuentes, A., Lasisi, T., Lee, S., McLean, S., & Nelson, R. (2019). *American Association of Physical Anthropology: Statement on Race & Racism*.

Allen, J. A. (1877). "The influence of Physical conditions in the genesis of species". *Radical Review*, 1: 108–140.

Anton, S.C. (1989). Intentional cranial vault deformation and induced changes of the cranial base and face. *American Journal of Physical Anthropology, 79:253–267.*

Bastir, M., Godoy, P., & Rosas, A. (2011). Common features of sexual dimorphism in the cranial airways of different human populations. *American Journal of Physical Anthropology,* 146, 414–422.

Belkhir, J. A., & Duyme, M. (1998). Intelligence and race, gender, class: The fallacy of genetic determinism; rethinking intelligence from the position of the oppressed. *Race, Gender & Class, 5*(3), 136.

Bergmann, C. (1847) Ueber die verhältnisse der wärmeökonomie der thiere zuihrer Grösse. *Göttinger Studien* 3: 595–708.

Blakey, M. L. (1999). Scientific racism and the biological concept of race. *Literature and Psychology, 45*(1), 29-43.

Buikstra, J. E., & Ubelaker, D. H. (1994). Standards for data collection from human skeletal remains: *Proceedings of a seminar at the Field Museum of Natural History*. Fayetteville: Arkansas Archeological Survey.

Butaric, L. N. (2015). Differential scaling patterns in maxillary sinus volume and nasal cavity breadth among modern humans. *The Anatomical Record*, 298, 1710–1721.

Butaric, L. N., & Klocke, R. P. (2018). Nasal variation in relation to high altitude adaptations among Tibetans and Andeans. *American Journal of Human Biology,* 30, e23104.

Carey, J. W., & Steegmann, J. T. (1981). Human nasal protrusion, latitude, and climate. *American Journal of Physical Anthropology*, 56, 313–319.

Cauna, N. (1982). Blood and nerve supply of the nasal lining. In D. F. Proctor, I. Andersen, (Eds.), *The nose: Upper airway physiology and the atmospheric environment* (pp. 45–69). New York: Elsevier Biomedical Press.

Charles, C. M. (1930). The cavum nasi of the American Negro. *American Journal of Physical Anthropology,* 14, 177–253.

Chierici G, Harrold EP, Vargervik K. (1973). Morphogenetic experiments in facial asymmetry: the nasal cavity. *American Journal of Physical Anthropology*, 38:291–300.

Churchill, S. E., Shackelford, L. L., Georgi, J. N., & Black, M. T. (2004). Morphological variation and airflow dynamics in the human nose. *American Journal of Human Biology,* 16, 625–638.

Cobzeanu, M., Bâldea, V., Bâldea, M., Vonica, P., & Cobzeanu, B. (2014). The anatomo-radiological study of unusual extrasinusal pneumatizations: Superior and supreme turbinate, crista galli process, uncinate process. *Romanian journal of morphology and embryology*. 55. 1099-104.

Cole, P. (1953a). Some aspects of temperature, moisture and heat relationships in the upper respiratory tract. *The Journal of Laryngology & Otology,* 67, 449–456.

Cole, P. (1953b). Further observations on the conditioning of respiratory air. *The Journal of Laryngology & Otology,* 67, 669–681.

Cole, P. (1954). Recordings of respiratory air temperature. *The Journal of Laryngology & Otology,* 68, 295–307.

Cole, P. (1982). Modification of inspired air. In D. F. Proctor & I. Andersen (Eds*.), The nose: Upper airway physiology and the atmospheric environment* (pp. 351–375). New York: Elsevier Biomedical Press.

Cole, P. (2000). Biophysics of nasal airflow: A review. *American Journal of Rhinology*, *14*(4), 245–249.

Corey, J. P., Gungor, A., Nelson, R., Liu, X. L., & Fredberg, J. (1998). Normative standards for nasal cross-sectional areas by race as measured by acoustic rhinometry. *Otolaryngology - Head and Neck Surgery,* 119, 389–393.

Crognier, E. (1981a). Climate and anthropometric variations in Europe and the Mediterranean area. *Annals of Human Biology*, 8, 99–107.

Crognier, E. (1981b). The influence of climate on the physical diversity of European and Mediterranean populations. *Journal of Human Evolution,* 10, 611–614.

Davies, A. (1932). A resurvey of the nose in relation to climate. *Journal of the Royal Anthropological Institute*, 62, 337–359.

Doorly, D. J., Taylor, D. J., & Schroter, R. C. (2008). Mechanics of airflow in the human nasal airways. *Respiratory Physiology & Neurobiology,*163, 100–110.

Earwaker, J. (1993). Anatomic variants in sinonasal CT. *Radiographics: A Review Publication of the Radiological Society of North America, Inc*, 13(2), 381–415.

Eccles, R. (2002). An explanation for the seasonality of acute upper respiratory tract viral infections. *Acta Oto-Laryngologica*, 122(2), 183–191.

Elad, D., Liebenthal, R., Wenig, B. L., & Einav, S. (1993). Analysis of airflow patterns in the human nose. *Medical & Biological Engineering & Computing,* 31, 585–592.

Elad, D., Wolf, M., & Keck, T. (2008). Air-conditioning in the human nasal cavity. *Respiratory Physiology & Neurobiology,* 163, 121–127.

Evteev, A., Cardini, A. L., Morozova, I., & O'Higgins, P. (2014). Extreme climate, rather than population history, explains mid-facial morphology of Northern Asians. *American Journal of Physical Anthropology,* 153, 449–462.

Evteev, A. A., & Movsesian, A. A. (2015). Testing the association between human mid-facial morphology and climate using autosomal, mitochondrial, Y chromosomal polymorphisms and cranial non-metrics. *American Journal of Physical Anthropology,* 159, 517–522.

Fedorov A., Beichel R., Kalpathy-Cramer J., Finet J., Fillion-Robin J-C., Pujol S., Bauer C., Jennings D., Fennessy F.M., Sonka M., Buatti J., Aylward S.R., Miller J.V., Pieper S., Kikinis R. (2019). 3D Slicer as an Image Computing Platform for the Quantitative Imaging Network. *Magnetic Resonance Imaging.* 30 (9), 1323–1341.

Franciscus, R. G., & Trinkaus, E. (1988). Nasal morphology and the emergence of Homo erectus. *American Journal of Physical Anthropology*, 75, 517–527.

Franciscus, R. G., & Long, J. C. (1991). Variation in human nasal height and breadth. *American Journal of Physical Anthropology*, 85, 419–427.

Franciscus, R. G. (1995). *Later Pleistocene nasofacial variation in western Eurasia and Africa and modern human origins*. Ph.D. thesis, University of New Mexico, Albuquerque.

Fukase, H., Ito, T., & Ishida, H. (2016). Geographic variation in nasal cavity form among three human groups from the Japanese Archipelago: Ecogeographic and functional implications. *American Journal of Human Biology,* 28, 343–351.

Gibelli, D., Cellina, M., Gibelli, S., Cappella, A., Oliva, A. G., Termine, G., & Sforza, C. (2018). Anatomical variants of ethmoid bone on multidetector CT. *Surgical and Radiologic Anatomy:* SRA, 40(11), 1301–1311.

Gravlee, C. C. (2009). How race becomes biology: Embodiment of social inequality. *American Journal of Physical Anthropology*, *139*(1), 47–57.

Hall, R. L. (2005). Energetics of nose and mouth breathing, body size, body composition, and nose volume in young adult males and females. *American Journal of Human Biology,* 17, 321–330.

Harvati, K., & Weaver, T. D. (2006). Human cranial anatomy and the differential preservation of population history and climate signatures. *The Anatomical Record. Part A, Discoveries in molecular, cellular, and evolutionary biology*, 288, 1225–1233.

Havenith, G. (2005). Temperature regulation, heat balance and climatic stress. In W. Kirch, B. Menne, & R. Bertollini (Eds.), *Extreme weather events and public health responses* (pp. 69–80). Berlin: Springer-Verlag.

Hildebrandt, T., Heppt, W. J., Kertzscher, U., & Goubergrits, L. (2013). The concept of rhinorespiratory homeostasis—A new approach to nasal breathing. *Facial Plastic Surgery*, 29(02), 085–092.

Holton, N. E., Alsamawi, A., Yokley, T. R., & Froehle, A. W. (2016). The ontogeny of nasal shape: An analysis of sexual dimorphism in a longitudinal sample. *American Journal of Physical Anthropology,* 160, 52–61.

Holton, N. E., Piche, A., & Yokley, T. R. (2018). Integration of the nasal complex: Implications for developmental and evolutionary change in modern humans. *American Journal of Physical Anthropology*, 166(4), 791–802.

Holton, N. E., Yokley, T. R., & Butaric, L. N. (2013). The morphological interaction between the nasal cavity and maxillary sinuses in living humans. *The Anatomical Record,* 296, 414–426.

Hubbe, M., Hanihara, T., & Harvati, K. (2009). Climate signatures in the morphological differentiation of worldwide modern human populations. *The Anatomical Record,* 292, 1720–1733.

Ingelstedt, S. (1970). Humidifying capacity of the nose. *Annals of Otolaryngology,* 79, 475–480.

Inthavong, K., Tian, Z. F., & Tu, J. Y. (2007). CFD simulations on the heating capability in a human nasal cavity. In P. Jacobs, T. McIntyre, M. Cleary, D. Buttsworth, R. Mee, R. Clements, R. Morgan, C. Lemckert (Eds.), *Proceedings of the 16th Australasian Fluid Mechanical Conference (AFMC).* Gold Coast, Queensland, Australia, p 842–847.

Keck, T., Leiacker, R., Riechelmann, H., & Rettinger, G. (2000a). Temperature profile in the nasal cavity. *Laryngoscope*, 110, 651–654.

Keck, T., Leiacker, R., Heinrich, A., Kühnemann, S., & Rettinger, G. (2000b). Humidity and temperature profile in the nasal cavity. *Rhinology*, 38, 167–171.

Keyhani, K. P. W. M. M., Scherer, P. W., & Mozell, M. M. (1995). Numerical simulation of airflow in the human nasal cavity. *Journal of Biomechanical Engineering*, 117(4), 429–441.

Kim, S. & Maddux, S. (2018). *Thermoregulation and the Human Nose: Balancing Climatic and Energetic Factors* [Abstract]. Research Appreciation Day 2018, UNT Health Science Center, Ft. Worth, TX, United States.

Lang, J. (1989). Clinical anatomy of the nose, nasal cavity and paranasal sinuses. New York: Thieme Medical Publishers, Inc.

Leong, S. C., & Eccles, R. (2009). A systematic review of the nasal index and the significance of the shape and size of the nose in rhinology. *Clinical Otolaryngology*, 34, 191–198.

Lindemann, J., Tsakiropoulou, E., Keck, T., Leiacker, R., & Wiesmiller, K. M. (2009). Nasal air conditioning in relation to acoustic rhinometry values. *The American Journal of Rhinology & Allergy*, 23, 575–577.

Maddux, S. D., Yokley, T. R., Svoma, B. M., & Franciscus, R. G. (2016). Absolute humidity and the human nose: A reanalysis of climate zones and their influence on nasal form and function. *American Journal of Physical Anthropology*, 161, 309–320.

Maddux, S. D., Butaric, L. N., Yokley, T. R., & Franciscus, R. G. (2017). Ecogeographic variation across morphofunctional units of the human nose. *American Journal of Physical Anthropology*, *162*(1), 103–119.

Mariak, Z., White, M. D., Lewko, J., Lyson, T., & Piekarski, P. (1999). Direct cooling of the human brain by heat loss from the upper respiratory tract. *Journal of Applied Physiology,* 87, 1609–1613.

Marks, T.N., Maddux, S.D., Butaric, L.N., Franciscus, R.G. (2019). Climatic adaptation in human inferior nasal turbinate morphology: Evidence from Arctic and equatorial populations. *American Journal of Physical Anthropology,* 169: 498– 512.

Maroldi, R., Borghesi, A., & Maculotti, P. (2005). CT and MR Anatomy of Paranasal Sinuses: Key Elements. In R. Maroldi & P. Nicolai (Eds.), *Imaging in Treatment Planning for Sinonasal Diseases* (pp. 9–27). Springer.

Márquez, S. (2008), The Paranasal Sinuses: The Last Frontier in Craniofacial Biology. *Anatomical Record*, 291: 1350-1361.

Meigs, J. A. (1857). *Catalogue of human crania, in the collection of the Academy of Natural Sciences of Philadelphia: Based upon the third edition of Dr. Morton's "catalogue of skulls"* (Vol. 8). Philadelphia: JB Lippincott & Company.

Mills, R. P., & Christmas, H. E. (1990). Applied comparative anatomy of the nasal turbinates. *Clinical Otolaryngology and Allied Science*, 15, 553–558.

Mlynski, G., Gr€utzenmacher, S., Plontke, S., Mlynski, B., & Lang, C. (2001). *Correlation of nasal morphology and respiratory function*. Rhinology, 39, 197–201.

Naftali, S., Rosenfeld, M., Wolf, M., & Elad, D. (2005). The air conditioning capacity of the human nose. *Annals of Biomedical Engineering*, 33, 545–553.

NCSS 11 Statistical Software. (2016). NCSS, LLC. Kaysville, UT, ncss.com/software/ncss.

Nicoleta, M., Rusu, M., & Săndulescu, M. (2015). Variant anatomy of nasal turbinates: Supreme, superior and middle conchae bullosae, paradoxical superior and inferior turbinates, and middle accessory turbinate. *Romanian Journal of Morphology and Embryology = Revue Roumaine de Morphologie et Embryologie*, *56*, 1223–1226.

Noback, M. L., Harvati, K., & Spoor, F. (2011). Climate-related variation of the human nasal cavity. *American Journal of Physical Anthropology*, 145, 599–614.

Psaltis, A. J., & Wormald, P.-J. (2019). Classification of Frontal Recess Cells and Extent of Surgery. In D. Lal & P. H. Hwang (Eds.), *Frontal Sinus Surgery: A Systematic Approach* (pp. 55–72). Springer International Publishing.

Ramachandran, S., Deshpade, O., Roseman, C. C., Rosenberg, N. A., Feldman, M. W., & Cavalli-Sforza, L. L. (2005). Support from the relationship of genetic and geographic distance in human populations for a serial found effect originating in Africa. *Proceedings of the National Academy of Sciences,* 102, 15942–15947.

.

Relethford, J. H. (2002). Apportionment of global human genetic diversity based on craniometrics and skin color. *American Journal of Physical Anthropology*, *118*(4), 393–398.

Relethford, J. H. (2009). Race and global patterns of phenotypic variation. *American Journal of Physical Anthropology*, 139(1), 16-22.

Renschler, E. S. (2007). *An osteobiography of an African diasporic skeletal sample: Integrating skeletal and historical information.* PhD dissertation. Philadelphia: University of Pennsylvania.

Sahin-Yilmaz, A., & Naclerio, R. M. (2011). Anatomy and Physiology of the Upper Airway. *Proceedings of the American Thoracic Society*, *8*(1), 31–39.

Schaefer, C. M., & Maddux, S. D. (2019). *Assessing ecogeographic variation in superior ethmoidal breadth as a proxy for internal airway dimensions* [Poster]. SOAR: Summer Opportunities in Anatomy Research 2019, UNT Health Science Center, Ft. Worth, TX, United States.

Schlager, S., & Rudell, A. (2015). Analysis of the human osseous nasal shape—population differences and sexual dimorphism. *American Journal of Physical Anthropology*, 157, 571–581.

Schmidt-Nielsen, K., Hainsworth, F. R., & Murrish, D. E. (1970). Countercurrent heat exchange in the respiratory passages: Effect on water and heat balance. *Respiration Physiology*, 9, 263–276.

Schroter, R. C., & Watkins, N. V. (1989). Respiratory heat exchange in mammals. *Respiration Physiology*, 78, 357–367.

Scott, J. H. (1954). Heat regulating function of the nasal mucous membrane. *The Journal of laryngology and otology, 68, 308–317.*

Segal, R. A., Kepler, G. M., & Kimbell, J. S. (2008). Effects of differences in nasal anatomy on airflow distribution: A comparison of four individuals at rest. *Annals of Biomedical Engineering*, 36, 1870–1882.

Serrat, M. A., Schlierf, T. J., Efaw, M. L., Shuler, F. D., Godby, J., Stanko, L. M., & Tamski, H. L. (2015). Unilateral heat accelerates bone elongation and lengthens extremities of growing mice. *Journal of Orthopaedic Research*, 33(5), 692–698.

Shusterman, D. (2002). Review of the Upper Airway, Including Olfaction, as Mediator of Symptoms. *Environmental Health Perspectives*, 110 (4) 649–653.

Thomson, A. (1913). The correlations of isotherms with variations in the nasal index. *International Congress of Medicine London*, 17, 89–90.

Thomson, A., & Buxton, L. H. D. (1923). Man's nasal index in relation to certain climatic conditions. *Journal of the Royal Anthropological Institute*, 53, 92–122.

Tos, M. (1982). Goblet cells and glands in the nose and paranasal sinuses. In D. F. Proctor, I. Andersen (Eds.), *The nose: Upper airway physiology and the atmospheric environment* (pp. 99–144). New York: Elsevier Biomedical Press.

Uliyanov, Y. P. (1998). Clinical manifestations of the variants of nasal aerodynamics. *Journal of Otolaryngology - Head & Neck Surgery,* 152,152–153.

Van Valkenburgh, B., Theodor, J., Friscia, A., Pollack, A., & Rowe, T. (2004). Respiratory turbinates of canids and felids: A quantitative comparison. Journal of Zoology, 264, 281–293.

Walker, J. E., Wells, R. E., & Merrill, E. W. (1961). Heat and water exchange in the respiratory tract. *The American Journal of Medicine*, *30*, 259–267.

Weiner, J. S. (1954). Nose shape and climate. *American Journal of Physical Anthropology,* 12, 615–618.

Wolf, M., Naftali, S., Schroter, R. C., & Elad, D. (2004). Air-conditioning characteristics of the human nose. *The Journal of Laryngology & Otology,* 118, 87–92.

Wolpoff, M. H. (1968). Climatic influence on the skeletal nasal aperture. *American Journal of Physical Anthropology, 2*9, 405–424.

Yokley, T. R. (2009). Ecogeographic variation in human nasal passages. *American Journal of Physical Anthropology*, *138*(1), 11–22.

Zaidi, A. A., Mattern, B. C., Claes, P., McEcoy, B., Hughes, C., & Shriver, M. D. (2017). Investigating the case of human nose shape and climate adaptation. *Public Library of Science Genetics*, *13*(3), e1006616.

Zhao, K., & Jiang, J. (2014). What is normal nasal airflow? A computational study of 22 healthy adults. *International Forum of Allergy & Rhinology*, 4, 435–446.

CURRICULUM VITAE

[redacted]

[redacted]

[redacted]